

000 001 002 003 004 005 006 007 008 009 010 WHEN MORE IS LESS: UNDERSTANDING CHAIN-OF- THOUGHT LENGTH IN LLMS

005 **Anonymous authors**

006 Paper under double-blind review

ABSTRACT

011 Large Language Models (LLMs) increasingly rely on Chain-of-Thought (CoT)
 012 reasoning to solve complex problems. Contrary to the common belief that longer
 013 CoTs always improve performance, we demonstrate that **longer is not always better**.
 014 Across both real-world LLMs and theoretical models, task accuracy follows an
 015 inverted U-shaped curve with respect to CoT length: performance rises initially but
 016 declines once reasoning chains become too long. Through controlled experiments,
 017 we uncover **scaling behaviors of the optimal CoT length**: it increases with task
 018 difficulty but decreases with model capability. This exposes a significant mismatch
 019 with current practice, where supervised training often reuses the same CoT data
 020 across models and tasks without adaptivity. We further show that Reinforcement
 021 Learning (RL) can mitigate this gap by dynamically calibrating CoT length, thereby
 022 improving accuracy and offering a new perspective on differences between su-
 023 pervised fine-tuning and RL training. To explain these phenomena, we introduce
 024 an error-accumulation analysis that characterizes how reasoning errors propagate
 025 across steps and derives the scaling behaviors of CoT length observed empirically.
 026 Building on these insights, we show that training with optimally sized CoTs and
 027 applying length-aware filtering during inference yields substantial improvements
 028 in performance. Taken together, these findings establish a principled explanation of
 029 the “overthinking” effect and yield practical guidelines for calibrating CoT length
 030 in accordance with task complexity and model capability.

1 INTRODUCTION

031 Large language models (LLMs) have demonstrated impressive capabilities in solving complex
 032 reasoning tasks (Brown et al., 2020; Touvron et al., 2023). A central technique enabling these
 033 advances is Chain-of-Thought (CoT) reasoning (Wei et al., 2022), where models generate explicit
 034 intermediate steps to decompose complex problems into simpler, more manageable sub-problems,
 035 akin to a divide-and-conquer strategy (Zhang et al., 2024).

036 A widely held intuition, supported by prior studies (Fu et al., 2023; Jin et al., 2024), is that longer and
 037 more detailed CoTs generally yield better performance, especially on difficult tasks. At the same
 038 time, recent evidence shows that concise CoTs can sometimes be more effective, though often with
 039 trade-offs on challenging problems (Nayab et al., 2024). This raises a fundamental question: *does*
 040 *reasoning performance consistently improve as CoTs grow longer, or is there an inherent limit?*

041 In this paper, we provide a comprehensive answer through evidence from real-world LLMs, synthetic
 042 experiments, and theoretical modeling. We show that for CoT reasoning, *longer is not always better*.
 043 As illustrated in Figures 1a and 1b, task accuracy typically follows an *inverted U-shaped* curve with
 044 respect to CoT length: performance improves when the chain appropriately decomposes the task,
 045 but deteriorates when the chain becomes excessively long (due to error accumulation) or too short
 046 (leaving individual steps overly complex). This reveals the existence of an **optimal CoT length** that
 047 balances these competing forces. Identifying and calibrating to this optimal length is crucial for
 048 building reasoning models that are both efficient and accurate.

049 To uncover the mechanisms underlying this optimality, we design controlled experiments on arithmetic
 050 and dynamic programming tasks, and identify clear scaling behaviors: (1) harder tasks generally
 051 require longer CoTs to reach peak performance, (2) more capable models often achieve their maximum
 052 accuracy with shorter CoTs, and (3) solving harder tasks at the optimal length involves tackling

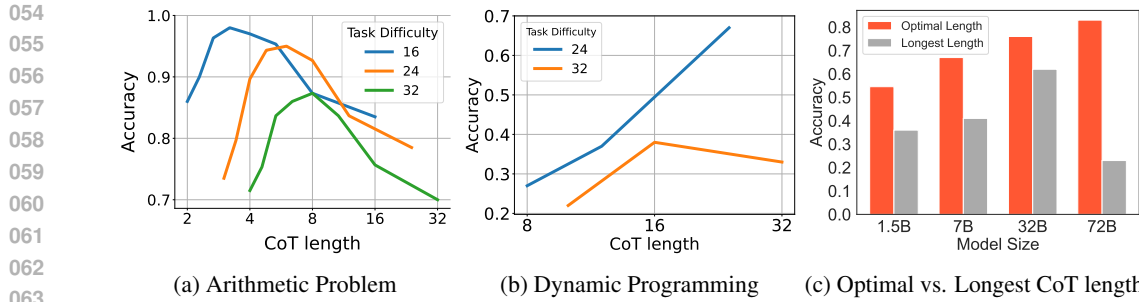


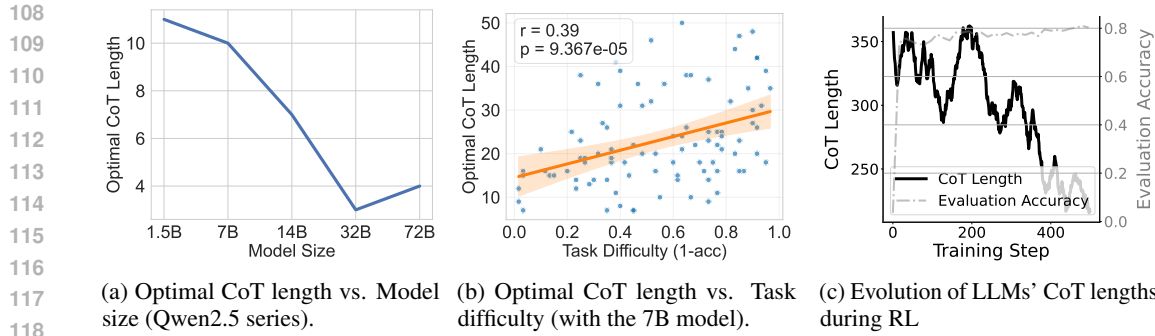
Figure 1: (a) Accuracy of a 6-layer GPT-2 on arithmetic tasks, showing inverted U-shaped curves with peaks shifting to longer CoTs as task difficulty increases. (b) Accuracy of a 5-layer GPT-2 on dynamic programming tasks, also following an inverted U-curve with respect to CoT length. (c) On the MMLU STEM dataset, CoTs of optimal length significantly outperform the longest CoTs.

increasingly difficult sub-tasks, motivating the need for adaptive reasoning strategies such as iterative or looping processes. Experiments on LLMs ranging from 1.5B to 72B parameters further confirm these trends. Together, these findings demonstrate that the optimal CoT length should adapt to both the problem and the model. As shown in Figure 1c, reasoning with the optimal length can significantly outperform the longest-possible CoTs (by more than 60% on a 72B model). In contrast, current practice often applies uniform CoT strategies across tasks and models during supervised learning, leading to systematic misspecification and suboptimal reasoning—sometimes causing larger models to perform worse than smaller ones. We further show that reinforcement learning (RL) can mitigate this gap by adaptively calibrating CoTs to their optimal lengths in pursuit of higher rewards. This sheds new light on why RL fine-tuning often yields superior reasoning performance and generalization compared to supervised learning (Huan et al., 2025).

To deepen our understanding, we develop a simple theoretical model based on an error-accumulation perspective: each model has a per-step success probability, so excessively long CoTs suffer from compounding errors, while overly short CoTs struggle with high per-step difficulty. This analysis not only explains the existence of an optimal length but also derives scaling laws that align closely with empirical observations. Extensions to nonlinear and stochastic error functions show the robustness of this perspective. At last, building on these insights, we demonstrate practical benefits: (i) training with optimally sized CoTs allows small models to outperform much larger ones trained on uniform-length data, and (ii) at inference time, filtering CoTs by estimated entropy yields consistent gains, improving majority-vote performance on LLaMA3-8B-Instruct and Qwen2.5-7B-Instruct.

In summary, our work makes the following contributions:

- **Longer is not always better.** We demonstrate the existence of an optimal CoT length across both real-world LLMs and synthetic tasks, challenging the prevailing intuition that performance monotonically improves with longer reasoning chains.
- **Scaling of optimal CoT length.** Through carefully controlled experiments, we systematically investigate how the optimal length depends on task difficulty and model capability, revealing consistent scaling laws: harder tasks require longer chains, while more capable models peak with shorter ones.
- **RL improves reasoning by calibrating CoT length.** We show that reinforcement learning adaptively steers CoT generation toward the optimal length, thereby explaining its superior reasoning performance compared to supervised finetuning.
- **An error-accumulation analysis.** We develop a simple yet useful theoretical model for understanding the observed CoT behaviors. From an error-accumulative perspective, This analysis explains the inverted U-shaped performance curve, derives the existence of an optimal CoT length, and recovers the observed scaling laws.
- **Practical implications.** We demonstrate actionable applications of our findings: (i) training with optimally sized CoT data enables smaller models to outperform larger ones trained with uniform-length chains, and (ii) a length-aware majority voting strategy that filters by entropy yields consistent gains at inference.



(a) Optimal CoT length vs. Model size (Qwen2.5 series). (b) Optimal CoT length vs. Task difficulty (with the 7B model). (c) Evolution of LLMs' CoT lengths during RL

Figure 2: Real-world observations of CoT length. (a) Larger models reach peak performance with shorter CoTs. (b) Harder tasks (lower baseline accuracy) require longer optimal CoTs, with a significant positive correlation ($p \ll 0.05$). (c) During RL training with GRPO on LeetCode-2K using Qwen2.5-7B-Instruct, average CoT length decreases as accuracy improves, suggesting that RL can also promote more efficient and concise reasoning paths.

Overall, our findings move beyond the assumption that “longer is better” and establish a principled foundation for calibrating CoT generation. By adapting to the optimal CoT length, we can develop LLMs that reason more effectively, avoiding both underthinking and counterproductive overthinking.

2 UNDERSTANDING COT LENGTHS IN REAL-WORLD LLMs

To ground our investigation in practical scenarios, we first examine the relationship between CoT length and reasoning performance in publicly available LLMs, and then study how reinforcement learning (RL) influences this relationship. We evaluate the Qwen2.5 series of Instruct models (Qwen et al., 2025) on the MMLU STEM benchmark, which contains challenging competition-level science and engineering problems (Hendrycks et al., 2021a). For each question, we generate 60 solutions spanning a wide range of lengths, where **CoT length is measured by the number of intermediate reasoning steps**. The *optimal CoT length* is defined as the one that yields the highest average accuracy. Additional details on step segmentation and length control are reported in Appendix D. To ensure diversity, we also consider tasks from **mathematics** (MATH), **science** (MMLU STEM), and **commonsense reasoning** (WinoGrande) across four different Qwen2.5-Instruct model sizes, though for clarity we present the MMLU STEM results in the main text and defer the rest to Appendix F.

Optimal Length Decreases with Stronger Model Capabilities: As depicted in Figure 2a, there is a clear trend where the optimal CoT length decreases as the model size increases. For instance, the optimal length shifts from 11, 10 steps for the 1.5B and 7B parameter model to 3, 4 steps for the 32B and 72B parameter model. This suggests that more capable models can consolidate reasoning into fewer, more potent steps, aligning with the Simplicity Bias concept where stronger models prefer shorter effective paths.

Optimal Length Grows with Harder Tasks: We also investigate how task difficulty influences the optimal CoT length. We use $(1 - \text{accuracy})$ on these questions as a proxy for the difficulty. Figure 2b shows a statistically significant positive correlation (notably $p = 1 \times 10^{-4} \ll 0.05$) between task difficulty and the optimal CoT length of Qwen2.5-7B-Instruct model. This indicates that more challenging problems will significantly benefit from a longer CoT with more extended decomposition steps. Similar trends for other models are provided in Appendix F.1.

RL does not always yield longer CoTs. A common belief in the development of advanced reasoning models is that reinforcement learning (RL) naturally produces longer reasoning traces. However, recent studies (Gandhi et al., 2025) suggest that the effect of RL on CoT length is strongly tied to the underlying base model, and that observed increases in length may reflect phenomena such as backtracking rather than genuinely deeper reasoning. To better understand this process, we monitor the evolution of CoT length during GRPO training (Shao et al., 2024) on LeetCode-2K (Xia et al., 2025) with Qwen2.5-7B-Instruct (Qwen et al., 2025). As shown in Figure 2c, optimizing outcome-based rewards can actually reduce the average response length as training converges. Consequently,

162 the RL-trained model produces shorter CoTs than its base counterpart on average, indicating that RL
 163 can exert mixed and non-monotonic influences on CoT length.
 164

165 3 A CONTROLLED STUDY OF COT LENGTH ON SYNTHETIC DATASETS

168 The real-world CoTs usually involve numerous uncontrolled variables (e.g., diverse reasoning
 169 strategies, planning, backtracking) and heterogeneous pre-training of base models, which makes
 170 precise mechanistic understanding difficult. To overcome these limitations and rigorously examine
 171 our hypotheses about optimal CoT length and Simplicity Bias, we design controlled synthetic
 172 experiments.

173 3.1 EXPERIMENTAL SETUP

175 **A Simple Arithmetic Problem.** Our first synthetic dataset consists of arithmetic problems involving
 176 sequences of addition operations. The intrinsic difficulty of a problem is quantified by the total
 177 number of addition operators, T . For each problem with T operators, we construct multiple valid
 178 CoT solutions that differ in length and granularity. The CoT length N is defined as the number
 179 of intermediate reasoning steps, where each step i processes t_i operators. For simplicity in this
 180 controlled study, we enforce $t_i \approx t$ across steps, where t denotes the step size (operators per step)
 181 and $N \approx T/t$.

182 For example, consider the problem "1+2+3+4+5+6+7", which contains $T = 6$ addition operators.
 183 We can construct different CoT solutions:

- 185 • A *long CoT solution* with $t = 1$ (one operator per step), yielding $N = 6$ steps:

186 Problem: 1+2+3+4+5+6+7
 187 Step 1: 1+2 = 3. (Remaining: 3+3+4+5+6+7)
 188 Step 2: 3+3 = 6. (Remaining: 6+4+5+6+7)
 189 ...
 190 Step 6: 21+7 = 28. (Final Answer)

- 192 • A *shorter CoT solution* with $t = 3$ (three operators per step), yielding $N = 2$ steps:

193 Problem: 1+2+3+4+5+6+7
 194 Step 1: 1+2+3+4 = 10. (Remaining: 10+5+6+7)
 195 Step 2: 10+5+6+7 = 28. (Final Answer)

198 This dataset design enables systematic variation of CoT length (N) and step size (t) for problems
 199 with fixed total difficulty (T). It allows us to isolate how the structure of the reasoning process itself
 200 influences performance. Additional details on problem formulation, data format, and CoT generation
 201 are provided in Appendix B.

202 **A Dynamic Programming Problem.** Beyond arithmetic tasks, we also consider a more general
 203 dynamic programming (DP) setting: the *Maximum Path Sum in a Number Triangle*, as studied in
 204 prior CoT theory (Feng et al., 2023). The objective is to find a path from the apex to the base that
 205 maximizes the sum. The canonical bottom-up DP algorithm solves this by iteratively updating values
 206 from the second-to-last row upward. By varying how many rows are merged in each update, we can
 207 directly control the effective CoT length while still guaranteeing correctness. This property makes the
 208 problem naturally decomposable into solutions of different lengths, closely mirroring the arithmetic
 209 case. Results on this DP task are consistent with our observations on arithmetic addition, further
 210 reinforcing the generality of the phenomena. For brevity, we focus on the arithmetic results in the
 211 main text and defer the DP experiments and details to Appendix C.

212 **Model and Training:** We train GPT-2 models (Radford et al., 2019) of varying depths (number
 213 of layers), keeping other hyperparameters fixed. Model depth is known to be a significant factor
 214 representing model capabilities for reasoning tasks (Ye et al., 2024; Chen et al., 2024a). Controlling
 215 this hyperparameter alone allows us to study the impact of model capability on optimal CoT length.
 Models are trained with CoT solutions that can be automatically synthesized for this task, with varying

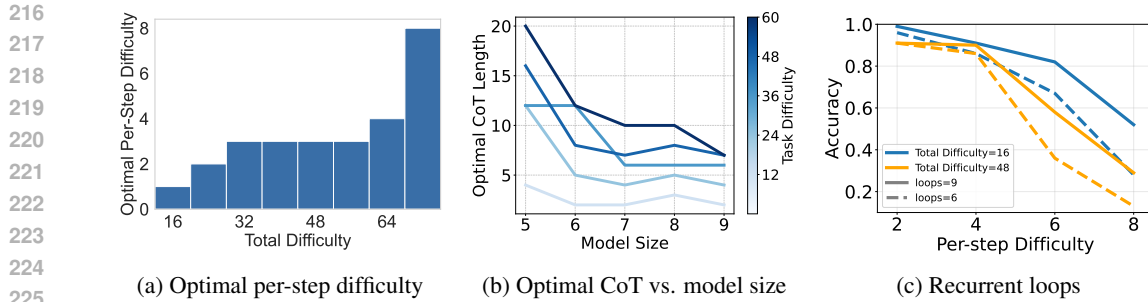


Figure 3: **CoT behaviors in synthetic experiments.** (a) Optimal per-step difficulty (t) increases with task difficulty, indicating that harder tasks require solving more complex sub-steps. (b) Optimal CoT length decreases with larger model size, while harder tasks require longer optimal CoTs at any fixed size. (c) Accuracy comparison between 6-loop and 9-loop models across task difficulties. As per-step difficulty grows, the performance gap widens, indicating that allocating additional loops, i.e., greater per-step reasoning effort, provides clear benefits on harder sub-problems.

total operators T and CoT lengths N (or equivalently the step sizes t). For testing, we can guide the model to produce a CoT of a specific length (e.g., by prompting with a control token indicating the desired number of operators t per step) or allow it to choose its preferred length. Further details are in Appendix H.

3.2 SCALING LAWS OF THE OPTIMAL COT LENGTH AND PRACTICAL INSIGHTS

Our controlled experiments not only corroborate the CoT behaviors observed in real-world scenarios but also allow for a more fine-grained analysis. These findings uncover several key scaling behaviors of the optimal CoT length that shed light into the practical designs of LLM reasoning.

I. Harder-Tasks' CoTs Peak at Longer Lengths (Adaptive CoT Length Matters): Our synthetic experiments further confirm the existence of an optimal CoT length, which manifests itself as an inverted U-shaped performance curve when plotting accuracy against the number of reasoning steps, as shown in Figure 1a and 1b. This clearly indicates that both "underthinking" (CoT too short) and "overthinking" (CoT too long) are detrimental, underscoring the critical benefit of generating CoTs with adaptive lengths tailored to the problem's demands. Moreover, we observe that the optimal CoT length shifts right as the task difficulty T gets larger, indicating that solving a harder task optimally requires a longer CoT (also observable numerically from Figure 3b). This suggests that a good reasoning model should be able to vary CoT lengths w.r.t. the overall task complexity.

II. Harder Tasks Peak at Harder Sub-tasks (Adaptive Per-Step Computation Helps): Figure 3a illustrates how the number of operators per step (t) impacts accuracy across different task difficulties (T). The envelope curve, tracing peak performance, shows that as tasks become harder (larger T), optimal accuracy is often achieved by CoTs that involve more complex computations *per step* (i.e., a larger optimal t^*). This indicates that for difficult problems, simply increasing the number of short, simple steps is insufficient—effective reasoning also requires increasing the complexity of the sub-tasks addressed at each step.

Implication on Model Choice. Current LLMs, with fixed Transformer depth, have limited ability to adapt their per-step computation, which constrains their reasoning strategies. In contrast, recent designs such as looped Transformers, which allow adaptive recurrent depth (Geiping et al., 2025; Chen et al., 2025), provide a mechanism to dynamically adjust per-step reasoning effort. This property directly aligns with the observed need for adaptive per-step computation.

To further validate this, we study looped Transformers where the same model can allocate more recurrent loops to increase reasoning effort at each step (Appendix E). Figure 3c plots accuracy against CoT length under fixed task complexity. As per-step difficulty increases, the performance gap between using 6 loops and 9 loops widens, showing that models benefit from allocating more reasoning effort (loops) when sub-tasks are harder. This finding highlights the importance of adaptive reasoning depth: looped Transformers should be trained not only to handle longer CoTs but also

270 to adjust their per-step computation according to task difficulty. To our knowledge, this direction
 271 remains underexplored but offers substantial potential for advancing reasoning performance.
 272

273 **III. Stronger Models Achieve Optimal Performance with Shorter CoTs (Model-Aware CoT**
 274 **Data Matter):** We also examine how model capability (number of layers) influences the optimal CoT
 275 length. Figure 3b indicates that, across different task complexities, the optimal number of CoT steps
 276 (N^*) consistently decreases as the model’s capability (number of layers) increases. This is because
 277 stronger models can effectively handle more complex sub-tasks in each step, thus requiring fewer
 278 overall steps to reach the solution optimally. This finding has significant implications for training
 279 data curation. It suggests that to achieve peak performance, models of different sizes or capabilities
 280 require CoT data tailored to their respective optimal per-step complexities. Current practices, such as
 281 using the same CoT datasets to train LLMs of varying sizes or directly distilling CoTs from large
 282 models to small ones without adapting complexity, may be suboptimal. For instance, a small model
 283 might struggle to learn effectively from overly complex CoT demonstrations designed for a larger
 284 model. Our analysis advocates for training each model with CoT data of adaptive complexity, aligned
 285 with its specific capabilities, to help it reach its optimal reasoning performance.

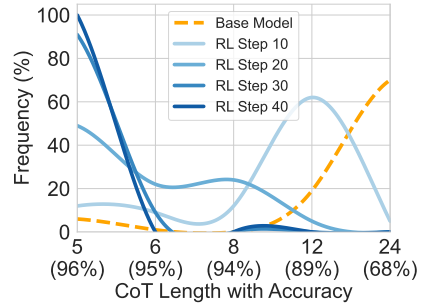
285 **IV. RL Training Converges to Optimal CoT Length**

286 **(RL Calibrates Reasoning Behaviors):** As discussed
 287 in Section 2, RL training of LLMs tends to shorten CoT
 288 length. Our synthetic experiments replicate this effect.
 289 Starting from a GPT-2 model pre-trained on CoT solutions
 290 of mixed lengths for a task with difficulty $T = 24$, we
 291 apply RL with rule-based outcome rewards using PPO on
 292 VERL (Schulman et al., 2017; Sheng et al., 2025). In our
 293 synthetic setup, each question comes with demonstrations
 294 of multiple CoT lengths, so the model naturally develops
 295 its own length preference. Figure 4 tracks how this
 296 preference shifts under RL, as reflected by the probability
 297 (shown on the y-axis) that the model spontaneously
 298 selects CoTs of different lengths. The base model spreads
 299 probability across lengths around 5, 12, and 24, but as
 300 RL training progresses, this distribution shifts to shorter
 301 CoTs and finally collapses toward the length 5, which is
 302 the accuracy-optimal length under controlled evaluation.

302 This demonstrates that RL, by directly optimizing task success, implicitly steers the model’s CoT
 303 generation policy toward the optimal length regime, thereby calibrating mismatches between training
 304 data and task-model requirements. From this viewpoint, the benefit of RL in LLM training extends
 305 beyond reward shaping or exploration: it also serves as an adaptive mechanism for aligning reasoning
 306 length. Even when the CoT data used in supervised learning is suboptimal (e.g., misaligned with task
 307 complexity or model capability), RL can automatically adjust the model’s behavior toward generating
 308 more effective, optimally sized CoTs.

309 **V. Self-Correction Training Shortens Optimal CoTs by Hardening Per-Step Reliability (Error-**
 310 **Tolerant Reasoning Improves Efficiency):** To study how self-correction interacts with optimal CoT
 311 length, we modify the training traces so that the model occasionally encounters an intentionally incor-
 312 rect intermediate result, immediately followed by a local repair. Concretely, instead of exposing the
 313 model only to clean chains of the form *question + step₁ + ans₁ + step₂ + ...*, we sometimes replace
 314 the first occurrence of a sub-result with a corrupted one and then show the corrected computation:
 315 *question + [step₁ + wrong_ans₁] (optionally) + step₁ + correct_ans₁ + step₂ + ...*. We control
 316 the fraction of such injected erroneous segments by a parameter p and, through preliminary sweeps,
 317 set $p = 0.3$, which strikes a balance between preserving core computational ability and providing
 318 sufficient exposure to local error repair. All other training configurations are kept fixed, and we train
 319 a 6-layer GPT-2 model under this setting.

320 At test time, we evaluate the model on arithmetic tasks of fixed difficulty and vary the CoT length,
 321 selecting the optimal length as the one that maximizes accuracy, as in our previous synthetic analyses.
 322 Importantly, when the model executes a self-correction within a single logical step, we count the
 323 original erroneous computation and its immediate correction as *one* CoT step, since our notion of
 324 CoT length reflects how finely the problem is decomposed, not how many times a local computation



324 Table 1: Optimal CoT length N^* and per-step difficulty t^* with and without self-correction (SC)
 325 across task difficulties T .

327 Task difficulty T	328 16	329 24	330 32	331 40
329 Optimal CoT length N^* w/o SC	4	5	8	10
330 Optimal CoT length N^* w/ SC	2	2	3	5
331 Optimal subtask difficulty t^* w/o SC	4	5	4	4
332 Optimal subtask difficulty t^* w/ SC	8	12	11	8

333 is revised. We then extract both the optimal number of steps N^* and the corresponding optimal
 334 per-step difficulty t^* (operators per step) across task difficulties $T \in \{16, 24, 32, 40\}$.

335 As shown in Table 1, self-correction training substantially reduces the optimal CoT length across
 336 all task difficulties (first two rows), while simultaneously shifting the optimal per-step difficulty to
 337 significantly larger values (last two rows). Although the shorter N^* might appear counter-intuitive
 338 given the extra “thinking” introduced during training, it is fully consistent with our broader picture:
 339 by learning to reliably repair local mistakes, the model becomes more robust to error accumulation
 340 within each step, which in turn allows it to tackle harder sub-tasks per step (larger t^*) without
 341 sacrificing accuracy. From a data-design perspective, these results suggest that injecting structured
 342 self-correction signals into CoT training can be an effective way to teach models to use fewer, but
 343 more powerful, steps.

345 4 AN ERROR ACCUMULATION ANALYSIS ON CHAIN-OF-THOUGHT

347 Empirical studies on both real-world and synthetic datasets consistently suggest the existence of an
 348 optimal Chain-of-Thought (CoT) length. To explain this, we develop a theoretical model based on
 349 an intuitive analysis of accumulated errors and extend it to more general settings. Remarkably, the
 350 predictions of this simple model align closely with the empirically observed scaling behaviors of CoT
 351 length in our toy model and large language models. While not exhaustive, these insights provide a
 352 useful lens for understanding and anticipating how CoT length influences reasoning performance. All
 353 proofs are deferred to Appendix J.

354 **Setup.** Consider the arithmetic task with T operators and an N -step CoT as in Section 3.1.
 355 At step i , the model produces a sub-question q_i and a sub-answer a_i , with history $H_{i-1} =$
 356 $[q_1, a_1, \dots, q_{i-1}, a_{i-1}]$. We use the likelihood factorization

$$357 P(a_{\text{final}}|q, \theta, N) = \prod_{i=1}^N \underbrace{P(q_i|H_{i-1}, q, \theta, N)}_{\text{sub-question}} \underbrace{P(a_i|q_i, H_{i-1}, q, \theta, N)}_{\text{sub-answer}},$$

360 We abstract diverse “reasoning behaviors” (reflection, verification, backtracking) as particular choices
 361 of task decomposition and focus on two error sources: (i) **sub-question error** $\sigma(T) \in [0, 1]$,
 362 increasing with difficulty T ; (ii) **sub-answer error** $E(N, M, T) \in [0, 1]$, depending on model
 363 capability M and effective per-step difficulty T/N . For each model with parameters θ , we define its
 364 capability $M(\theta)$ using the *reasoning boundary* (Chen et al., 2024b):

$$366 M = M(\theta) = \max_t \{ \Pr(a_i = a_i^* | t_i, \theta) > \varepsilon, |t_i| = t \},$$

368 where $|t_i|$ is the number of operators in the subtask t_i . Intuitively, $M(\theta)$ represents the largest
 369 sub-problem size the model can reliably solve in a single reasoning step.

371 **Proposition 4.1.** *Assuming stepwise stationarity and independence conditioned on history, the final
 372 accuracy takes the form*

$$373 A(N) = P(a_{\text{final}} = a_{\text{final}}^* | q, \theta, N) = \alpha \left((1 - \sigma(T))(1 - E(N, M, T)) \right)^N, \quad (1)$$

375 where α denotes a constant independent of N .

376 **A solvable special case.** For intuition, consider a linear sub-question error rate $\sigma(T) = \frac{T}{C}$, where
 377 C denotes the maximum task difficulty the model family is trained to handle, which is the largest

operator count present in the training distribution (with $T/C \leq 0.9$ within the training regime). Similarly, assume a linear sub-answer error $E(N, M, T) = T/(NM)$, which captures the number of operators processed per step relative to the model's capability M . Then

$$A(N) = \alpha \left(1 - \frac{T}{C}\right)^N \left(1 - \frac{T}{NM}\right)^N, \quad (2)$$

which increases for small N (decomposition helps) and decreases for large N (errors accumulate).

Theorem 4.2 (Optimal CoT length). *There exists an optimal $N^*(M, T)$ maximizing $A(N)$:*

$$N^*(M, T) = \frac{TZ}{M(Z+1)}, \quad Z = W_{-1}\left(-\left(1 - \frac{T}{Ce}\right)\right),$$

where W_{-1} is the negative branch of the Lambert W function ($we^w = x$).

This theorem establishes the inverted U-shaped relationship between CoT length and accuracy, and provides an explicit formula for the optimal length N^* . From this expression, we can formally derive the first three scaling behaviors characterized in Section 3.2.

Corollary 4.3 (Scaling laws). *From Theorem 4.2:*

- $N^*(M, T)$ increases with T (harder tasks warrant longer CoT).
- The optimal operators per step $t^* = T/N^*(M, T) = M(1 + 1/Z)$ increases with T (envelope behavior).
- $N^*(M, T)$ decreases with M (stronger models need fewer steps).

How RL Calibrates CoT. The same analysis also sheds light on why reinforcement learning (RL) with outcome supervision help calibrates CoT length (Section 3.2). During RL, the choice of CoT length can be viewed as selecting an action N_i from a discrete set $\mathcal{A} = \{N_1, \dots, N_k\}$. Each N_i produces a binary reward $r \in \{0, 1\}$ with success probability $A(N_i)$ from Proposition 4.1, reducing the setting to a stateless bandit. With a softmax policy $\pi_\theta(N_i) = \frac{e^{\theta_i}}{\sum_j e^{\theta_j}}$, the RL objective is

$$J(\theta) = \sum_{i=1}^k \pi_\theta(N_i) A(N_i), \quad \nabla_{\theta_i} J = \sum_{j=1}^k A(N_j) \pi_\theta(N_j) (\delta_{ij} - \pi_\theta(N_i)).$$

Corollary 4.4 (RL Converges to Optimal CoT Length). *For gradient ascent on $J(\theta)$ with sufficiently small step size, the policy converges to a deterministic solution $\pi_\theta(N_i) = 1$ iff $i = \arg \max_j A(N_j)$. Thus, RL training converges to the optimal CoT length $N^* = \arg \max_{N \in \mathcal{A}} A(N)$.*

This result shows that RL will automatically prefer the optimal length and hence calibrates the CoT length. In this way, our framework unifies the explanation of optimal CoT length, its scaling laws, and RL's calibration effects of reasoning lengths.

Extension to Nonlinear and Stochastic Error Functions. In the analysis above, we adopted a simple linear model with a closed-form solution for the optimal length to provide intuitive understanding. This framework can be extended to more general settings, including **nonlinear error functions** that are monotone and convex, as well as **stochastic error models** where each subtask may exhibit a different error rate. These extensions introduce additional technical subtleties but follow the same underlying principles. Overall, it shows that the accumulative error analysis can explain a broad class of reasoning process, including the arithmetic and dynamic programming problems we covered in Section 3. Due to space limitations, we defer the formal treatment to Appendix I.

5 PRACTICAL APPLICATIONS OF OPTIMAL COT LENGTH

Guided by the understanding above, in this section, we illustrate via some proof-of-concept experiments that adapting LLM training and inference configurations to the optimal CoT length can improve the model's reasoning performance.

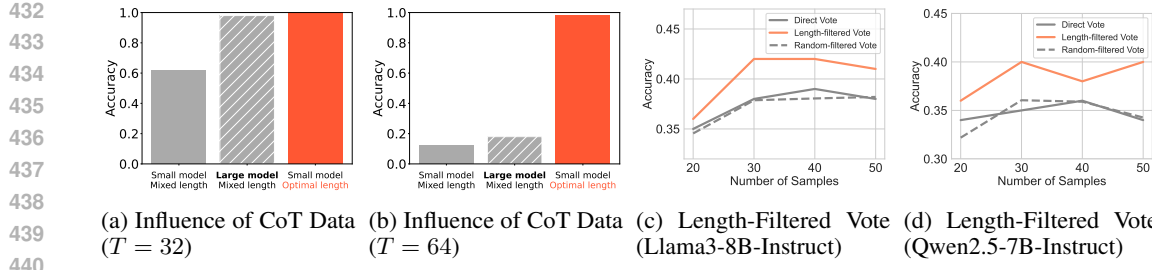


Figure 5: (a) and (b) compare model performance under different pretraining data distributions: Mixed Length (uniform over all lengths) vs. Optimal Length (only optimal-length solutions). Despite its smaller size, the small (6 layer) model trained on optimal-length data outperforms the large (9 layer) model trained on mixed-length data, with the performance gap widening as task difficulty increases. (c) and (d) validate our Length-Filtered Vote method on different models, which consistently outperforms vanilla majority vote and random-filtered vote on the GPQA dataset, maintaining strong performance even as the number of samples increases.

5.1 TRAINING WITH DATA OF OPTIMAL COT LENGTH

Training with Optimal-Length CoT Data: The existence of an adaptive, optimal CoT length suggests that one should design the CoT training data adaptively to fully optimize the model’s reasoning performance. To examine the influence of the CoT length of the training data, we train a model on a specialized dataset that contains CoT solutions with lengths known to be optimal for the given model size and task difficulty (T). We compare this model against a baseline model trained on a dataset of CoT solutions with uniformly distributed step lengths t . During testing, models were allowed to freely choose their CoT strategy.

Results. As shown in Figures 5a and 5b, the model trained on optimal-length CoTs significantly outperforms the models trained on mixed-length solutions. Remarkably, a smaller model (e.g., 6 layers) trained on optimal-length data can even outperform a larger model (e.g., 9 layers) trained on randomly chosen CoT lengths. This proof-of-concept experiment underscores the critical influence of the suitability of the CoT length in training data for the model. While it is generally hard to exactly estimate optimal CoT lengths in real-world problems, our theoretical and empirical studies provide valuable guidelines for a coarse estimate. We leave more in-depth studies to future work.

5.2 ADAPTIVE LENGTH-FILTERED VOTE AT INFERENCE TIME

The observation that CoTs of optimal length yield higher accuracy suggests that inference-time strategies could benefit from this insight. Standard approaches like majority voting over multiple sampled CoTs, such as self-consistency (Wang et al., 2023), treat all valid reasoning paths equally, regardless of their length. However, paths that are too short (underthinking) or too long (overthinking and error-prone) may contribute noisy or incorrect answers to the voting pool.

While Fu et al. (2023) previously proposed filtering out short CoTs, it worked for smaller 2023-era models where “longer is better.” Inspired by our findings, we propose **Length-Filtered Vote**, an adaptive method that enhances standard majority voting by preferentially weighting or exclusively considering answers derived from CoTs whose lengths fall within a proper range. Specifically, in majority vote, given a model f_θ , a question q , a ground truth answer a^* , we first sample a set of answer candidates $c_1, \dots, c_n \stackrel{i.i.d.}{\sim} f_\theta(q)$ independently. After that, instead of a direct vote, we group the answers by their corresponding CoT length $\ell(c_i)$ (discussed in Appendix D) into groups with equal bin size D (by default, we set $D = 2$), denoted as $\{L_j\}_{j=1}^m$. As our theory suggests that the prediction accuracy is peaked around a certain range of CoT length, we identify such groups through the prediction uncertainty of the answers within each group, based on the intuition that lower uncertainty implies better predictions. Specifically, we calculate the Shannon entropy $H(L_i)$ of the final answers given by the CoT chains in each group L_i . We use a majority vote only for the K (by default, we set $K = 3$) groups with the smallest entropy. For **Random-filtered Vote**, we do a random grouping of samples (i.e., not based on length), and repeat the same entropy-based filtering process,

486 averaging the final results over 100 trials to account for the randomness of the grouping. A detailed
 487 description of the algorithm is in Appendix K.
 488

489 **Results.** We evaluate the proposed method against vanilla majority vote (i.e., self-consistency (Wang
 490 et al., 2023)) on a randomly chosen subset from the GPQA dataset (Rein et al., 2023). The results
 491 in Figure 5c and 5d show that our filtered vote consistently outperforms vanilla majority vote and
 492 random-filtered vote and shows little performance degradation as the sample number increases. In
 493 summary, our findings show that **CoT length, as one of the most easily computable feature in**
 494 **scenarios where token-level probabilities are unavailable, is correlated with the final accuracy.**

495 6 RELATED WORK

496 **Chain-of-Thought for LLM Reasoning.** CoT has become a core technique for LLMs to solve
 497 complex reasoning tasks by generating intermediate steps (Wei et al., 2022). Numerous variants arise
 498 to enhance CoT reasoning with more structural substeps, such as least-to-most prompting (Zhou
 499 et al., 2023), tree of Thoughts (Yao et al., 2023), and divide-and-conquer methods (Zhang et al., 2024;
 500 Meng et al., 2024). These methods fundamentally treat CoT as a framework for task decomposition
 501 and subtask solving that falls in our analysis in Section 4.

502 **Overthinking in CoT Reasoning.** With the rise of powerful reasoning models like OpenAI o1,
 503 scaling test-time compute with long CoT has gained prominence (Snell et al., 2024; Chen et al.,
 504 2024d; Wu et al., 2024; Brown et al., 2024). These studies often suggest that more computation like
 505 longer CoT can lead to better results. However, this is not always true. With similar interests as
 506 ours, a few concurrent works also investigated the “overthinking” phenomenon (Chen et al., 2024c)
 507 where reasoning models generate excessively long CoTs for simple problems and proposed some
 508 mitigation strategies Han et al. (2024); Luo et al. (2025); Ma et al. (2025); Sui et al. (2025). Our
 509 analysis goes beyond these observations by formally establishing the existence of an optimal CoT
 510 length and its scaling behaviors. Supported by both controlled experiments and theoretical analysis,
 511 it offers principled guidelines for designing more effective CoT strategies.

512 **Theoretical Understanding of CoT.** Numerous studies aim to theoretically formalize the Chain-of-
 513 Thought (CoT) process and understand its effectiveness. They include analyzing CoT’s computational
 514 advantages via circuit complexity (Feng et al., 2023; Li et al., 2024), and quantifying step-wise
 515 information gain from an information-theoretic standpoint (Ton et al., 2024). While Schaeffer et al.
 516 (2023) uses error accumulation to explain emergent abilities via a monotonic p^L formulation with
 517 fixed reasoning length, our work is the first to leverage error accumulation to analyze the influence of
 518 CoT length. In addition, Bao et al. (2024) and FU et al. (2025) identify and characterize the latent
 519 causal structures and robustness of model reasoning. Ye et al. (2024) conducted controlled synthetic
 520 experiments to help uncover underlying problem-solving mechanisms in LLMs. While Jiang et al.
 521 (2025) presents an automated framework that converts sequential Long CoTs into hierarchical tree
 522 structures. Distinct from these varied theoretical explorations, our findings on CoT scaling behaviors
 523 and the consequent need for model-specific CoT structures (as discussed in Section 3.2) resonate
 524 with the concept of algorithmic alignment (Xu et al., 2019), which suggests that models perform best
 525 when the problem structure aligns with their computational structure.

526 7 CONCLUSION

527 This work revisits a prevailing assumption in reasoning with large language models: that longer Chain-
 528 of-Thoughts (CoTs) are always better. Through controlled experiments and theoretical analysis, we
 529 showed that accuracy instead follows an inverted U-shaped curve with respect to CoT length, revealing
 530 the existence of an optimal length that balances finer task decomposition against compounding errors.
 531 Our systematic study further uncovered scaling behaviors of this optimal length across task difficulty,
 532 model size, per-step computation, and RL training.

533 Building on these insights, we demonstrated that training with optimally sized CoTs improves
 534 performance, and introduced *Length-Filtered Vote* as an effective inference strategy. Together, these
 535 findings highlight the importance of calibrating reasoning length rather than adopting a one-size-fits-
 536 all approach. We advocate for a principled framework in which LLMs adaptively allocate the right
 537 amount of reasoning effort, ultimately leading to more reliable and efficient problem solving.

540
Ethics Statement. This work complies with the ICLR Code of Ethics. While our methods are
 541 general, they may be applied in contexts with societal implications, including risks related to bias,
 542 fairness, and privacy. We encourage responsible use and declare no conflicts of interest.
 543

544 **Reproducibility.** We provide detailed descriptions of our methodology, datasets, model configura-
 545 tions, and evaluation metrics in both the main text and the Appendix. In addition, the complete source
 546 code is included in the supplementary materials to facilitate reproducibility.
 547

548 REFERENCES

549 Sangmin Bae, Adam Fisch, Hrayr Harutyunyan, Ziwei Ji, Seungyeon Kim, and Tal Schuster. Relaxed
 550 recursive transformers: Effective parameter sharing with layer-wise lora, 2025. URL <https://arxiv.org/abs/2410.20672>.
 551

553 Guangsheng Bao, Hongbo Zhang, Cunxiang Wang, Linyi Yang, and Yue Zhang. How likely do llms
 554 with cot mimic human reasoning?, 2024. URL <https://arxiv.org/abs/2402.16048>.
 555

555 Bradley Brown, Jordan Juravsky, Ryan Ehrlich, Ronald Clark, Quoc V. Le, Christopher Ré, and
 556 Azalia Mirhoseini. Large language monkeys: Scaling inference compute with repeated sampling,
 557 2024. URL <https://arxiv.org/abs/2407.21787>.
 558

559 Tom Brown, Benjamin Mann, Nick Ryder, Melanie Subbiah, Jared D Kaplan, Prafulla Dhari-
 560 wal, Arvind Neelakantan, Pranav Shyam, Girish Sastry, Amanda Askell, Sandhini Agar-
 561 wal, Ariel Herbert-Voss, Gretchen Krueger, Tom Henighan, Rewon Child, Aditya Ramesh,
 562 Daniel Ziegler, Jeffrey Wu, Clemens Winter, Chris Hesse, Mark Chen, Eric Sigler, Ma-
 563 teusz Litwin, Scott Gray, Benjamin Chess, Jack Clark, Christopher Berner, Sam McCan-
 564 dlish, Alec Radford, Ilya Sutskever, and Dario Amodei. Language models are few-shot
 565 learners. In H. Larochelle, M. Ranzato, R. Hadsell, M.F. Balcan, and H. Lin (eds.), *Ad-
 566 vances in Neural Information Processing Systems*, volume 33, pp. 1877–1901. Curran Asso-
 567 ciates, Inc., 2020. URL https://proceedings.neurips.cc/paper_files/paper/2020/file/1457c0d6bfcb4967418bfb8ac142f64a-Paper.pdf.
 568

569 Lijie Chen, Binghui Peng, and Hongxun Wu. Theoretical limitations of multi-layer transformer,
 570 2024a. URL <https://arxiv.org/abs/2412.02975>.
 571

571 Qiguang Chen, Libo Qin, Jiaqi WANG, Jingxuan Zhou, and Wanxiang Che. Unlocking the capabilities
 572 of thought: A reasoning boundary framework to quantify and optimize chain-of-thought. In
 573 *The Thirty-eighth Annual Conference on Neural Information Processing Systems*, 2024b. URL
 574 <https://openreview.net/forum?id=pC44UMwy2v>.
 575

576 Xingyu Chen, Jiahao Xu, Tian Liang, Zhiwei He, Jianhui Pang, Dian Yu, Linfeng Song, Qiuwei
 577 Liu, Mengfei Zhou, Zhuosheng Zhang, Rui Wang, Zhaopeng Tu, Haitao Mi, and Dong Yu.
 578 Do not think that much for 2+3=? on the overthinking of o1-like llms, 2024c. URL <https://arxiv.org/abs/2412.21187>.
 579

580 Yanxi Chen, Xuchen Pan, Yaliang Li, Bolin Ding, and Jingren Zhou. A simple and provable scaling
 581 law for the test-time compute of large language models, 2024d. URL <https://arxiv.org/abs/2411.19477>.
 582

583 Yilong Chen, Junyuan Shang, Zhenyu Zhang, Yanxi Xie, Jiawei Sheng, Tingwen Liu, Shuohuan Wang,
 584 Yu Sun, Hua Wu, and Haifeng Wang. Inner thinking transformer: Leveraging dynamic depth scaling
 585 to foster adaptive internal thinking, 2025. URL <https://arxiv.org/abs/2502.13842>.
 586

587 Karl Cobbe, Vineet Kosaraju, Mohammad Bavarian, Mark Chen, Heewoo Jun, Lukasz Kaiser,
 588 Matthias Plappert, Jerry Tworek, Jacob Hilton, Reiichiro Nakano, Christopher Hesse, and John
 589 Schulman. Training verifiers to solve math word problems, 2021. URL <https://arxiv.org/abs/2110.14168>.
 590

591 Guhao Feng, Bohang Zhang, Yuntian Gu, Haotian Ye, Di He, and Liwei Wang. Towards revealing
 592 the mystery behind chain of thought: A theoretical perspective. In *Thirty-seventh Conference on
 593 Neural Information Processing Systems*, 2023. URL <https://openreview.net/forum?id=qHrADgAdYu>.
 594

594 Yao Fu, Hao Peng, Ashish Sabharwal, Peter Clark, and Tushar Khot. Complexity-based prompting
 595 for multi-step reasoning, 2023. URL <https://arxiv.org/abs/2210.00720>.
 596

597 Zhizhang FU, Guangsheng Bao, Hongbo Zhang, Chenkai Hu, and Yue Zhang. Correlation or
 598 causation: Analyzing the causal structures of llm and lrm reasoning process, 2025. URL <https://arxiv.org/abs/2509.17380>.
 599

600 Kanishk Gandhi, Ayush Chakravarthy, Anikait Singh, Nathan Lile, and Noah D. Goodman. Cognitive
 601 behaviors that enable self-improving reasoners, or, four habits of highly effective stars, 2025. URL
 602 <https://arxiv.org/abs/2503.01307>.
 603

604 Jonas Geiping, Sean McLeish, Neel Jain, John Kirchenbauer, Siddharth Singh, Brian R Bartoldson,
 605 Bhavya Kailkhura, Abhinav Bhatele, and Tom Goldstein. Scaling up test-time compute with latent
 606 reasoning: A recurrent depth approach. *arXiv preprint arXiv:2502.05171*, 2025.
 607

608 Daya Guo, Dejian Yang, Haowei Zhang, Junxiao Song, Ruoyu Zhang, Runxin Xu, Qihao Zhu,
 609 Shirong Ma, Peiyi Wang, Xiao Bi, et al. Deepseek-r1: Incentivizing reasoning capability in llms
 610 via reinforcement learning. *arXiv preprint arXiv:2501.12948*, 2025.
 611

612 Tingxu Han, Zhenting Wang, Chunrong Fang, Shiyu Zhao, Shiqing Ma, and Zhenyu Chen. Token-
 613 budget-aware llm reasoning. *arXiv preprint arXiv:2412.18547*, 2024.
 614

615 Dan Hendrycks, Collin Burns, Steven Basart, Andy Zou, Mantas Mazeika, Dawn Song, and Jacob
 616 Steinhardt. Measuring massive multitask language understanding. In *International Conference on Learning Representations*, 2021a. URL <https://openreview.net/forum?id=d7KBjmI3GmQ>.
 617

618 Dan Hendrycks, Collin Burns, Saurav Kadavath, Akul Arora, Steven Basart, Eric Tang, Dawn Song,
 619 and Jacob Steinhardt. Measuring mathematical problem solving with the math dataset, 2021b.
 620 URL <https://arxiv.org/abs/2103.03874>.
 621

622 Maggie Huan, Yuetai Li, Tuney Zheng, Xiaoyu Xu, Seungone Kim, Minxin Du, Radha Pooven-
 623 dran, Graham Neubig, and Xiang Yue. Does math reasoning improve general llm capabilities?
 624 understanding transferability of llm reasoning. *arXiv preprint arXiv:2507.00432*, 2025.
 625

626 Gangwei Jiang, Yahui Liu, Zhaoyi Li, Wei Bi, Fuzheng Zhang, Linqi Song, Ying Wei, and Defu
 627 Lian. What makes a good reasoning chain? uncovering structural patterns in long chain-of-thought
 628 reasoning. In Christos Christodoulopoulos, Tanmoy Chakraborty, Carolyn Rose, and Violet
 629 Peng (eds.), *Proceedings of the 2025 Conference on Empirical Methods in Natural Language
 Processing*, pp. 6501–6525, Suzhou, China, November 2025. Association for Computational
 630 Linguistics. ISBN 979-8-89176-332-6. doi: 10.18653/v1/2025.emnlp-main.329. URL <https://aclanthology.org/2025.emnlp-main.329/>.
 631

632 Mingyu Jin, Qinkai Yu, Dong Shu, Haiyan Zhao, Wenyue Hua, Yanda Meng, Yongfeng Zhang,
 633 and Mengnan Du. The impact of reasoning step length on large language models. In *Annual
 634 Meeting of the Association for Computational Linguistics*, 2024. URL <https://api.semanticscholar.org/CorpusID:266902900>.
 635

636 Zhiyuan Li, Hong Liu, Denny Zhou, and Tengyu Ma. Chain of thought empowers transformers to
 637 solve inherently serial problems, 2024. URL <https://arxiv.org/abs/2402.12875>.
 638

639 Hunter Lightman, Vineet Kosaraju, Yura Burda, Harri Edwards, Bowen Baker, Teddy Lee, Jan
 640 Leike, John Schulman, Ilya Sutskever, and Karl Cobbe. Let's verify step by step, 2023. URL
 641 <https://arxiv.org/abs/2305.20050>.
 642

643 Haotian Luo, Li Shen, Haiying He, Yibo Wang, Shiwei Liu, Wei Li, Naiqiang Tan, Xiaochun Cao,
 644 and Dacheng Tao. O1-pruner: Length-harmonizing fine-tuning for o1-like reasoning pruning.
 645 *arXiv preprint arXiv:2501.12570*, 2025.
 646

647 Xinyin Ma, Guangnian Wan, Runpeng Yu, Gongfan Fang, and Xinchao Wang. Cot-valve: Length-
 648 compressible chain-of-thought tuning. *arXiv preprint arXiv:2502.09601*, 2025.

648 Zijie Meng, Yan Zhang, Zhaopeng Feng, and Zuozhu Liu. Dcr: Divide-and-conquer reasoning for
 649 multi-choice question answering with llms, 2024. URL <https://arxiv.org/abs/2401.05190>.

650

651 Sania Nayab, Giulio Rossolini, Giorgio Buttazzo, Nicolamaria Manes, and Fabrizio Giacomelli.
 652 Concise thoughts: Impact of output length on llm reasoning and cost, 2024. URL <https://arxiv.org/abs/2407.19825>.

653

654 Qwen, ;, An Yang, Baosong Yang, Beichen Zhang, Binyuan Hui, Bo Zheng, Bowen Yu, Chengyuan
 655 Li, Dayiheng Liu, Fei Huang, Haoran Wei, Huan Lin, Jian Yang, Jianhong Tu, Jianwei Zhang,
 656 Jianxin Yang, Jiaxi Yang, Jingren Zhou, Junyang Lin, Kai Dang, Keming Lu, Keqin Bao, Kexin
 657 Yang, Le Yu, Mei Li, Mingfeng Xue, Pei Zhang, Qin Zhu, Rui Men, Runji Lin, Tianhao Li, Tianyi
 658 Tang, Tingyu Xia, Xingzhang Ren, Xuancheng Ren, Yang Fan, Yang Su, Yichang Zhang, Yu Wan,
 659 Yuqiong Liu, Zeyu Cui, Zhenru Zhang, and Zihan Qiu. Qwen2.5 technical report, 2025. URL
 660 <https://arxiv.org/abs/2412.15115>.

661

662 Alec Radford, Jeffrey Wu, Rewon Child, David Luan, Dario Amodei, Ilya Sutskever, et al. Language
 663 models are unsupervised multitask learners. *OpenAI blog*, 1(8):9, 2019.

664

665 David Rein, Betty Li Hou, Asa Cooper Stickland, Jackson Petty, Richard Yuanzhe Pang, Julien Dirani,
 666 Julian Michael, and Samuel R. Bowman. Gpqa: A graduate-level google-proof q&a benchmark,
 667 2023. URL <https://arxiv.org/abs/2311.12022>.

668

669 Keisuke Sakaguchi, Ronan Le Bras, Chandra Bhagavatula, and Yejin Choi. Winogrande: An
 670 adversarial winograd schema challenge at scale, 2019. URL <https://arxiv.org/abs/1907.10641>.

671

672 Rylan Schaeffer, Brando Miranda, and Sanmi Koyejo. Are emergent abilities of large language
 673 models a mirage? In *Thirty-seventh Conference on Neural Information Processing Systems*, 2023.
 674 URL <https://openreview.net/forum?id=ITw9edRD1D>.

675

676 John Schulman, Filip Wolski, Prafulla Dhariwal, Alec Radford, and Oleg Klimov. Proximal policy
 677 optimization algorithms, 2017. URL <https://arxiv.org/abs/1707.06347>.

678

679 Zhihong Shao, Peiyi Wang, Qihao Zhu, Runxin Xu, Junxiao Song, Xiao Bi, Haowei Zhang,
 680 Mingchuan Zhang, Y. K. Li, Y. Wu, and Daya Guo. Deepseekmath: Pushing the limits of
 681 mathematical reasoning in open language models, 2024. URL <https://arxiv.org/abs/2402.03300>.

682

683 Guangming Sheng, Chi Zhang, Zilingfeng Ye, Xibin Wu, Wang Zhang, Ru Zhang, Yanghua Peng,
 684 Haibin Lin, and Chuan Wu. Hybridflow: A flexible and efficient rlhf framework. In *Proceedings of the Twentieth European Conference on Computer Systems*, EuroSys '25, pp. 1279–1297.
 685 ACM, March 2025. doi: 10.1145/3689031.3696075. URL <http://dx.doi.org/10.1145/3689031.3696075>.

686

687 Charlie Snell, Jaehoon Lee, Kelvin Xu, and Aviral Kumar. Scaling llm test-time compute optimally
 688 can be more effective than scaling model parameters, 2024. URL <https://arxiv.org/abs/2408.03314>.

689

690 Yang Sui, Yu-Neng Chuang, Guanchu Wang, Jiamu Zhang, Tianyi Zhang, Jiayi Yuan, Hongyi Liu,
 691 Andrew Wen, Shaochen Zhong, Hanjie Chen, et al. Stop overthinking: A survey on efficient
 692 reasoning for large language models. *arXiv preprint arXiv:2503.16419*, 2025.

693

694 Jean-Francois Ton, Muhammad Faaiz Taufiq, and Yang Liu. Understanding chain-of-thought in llms
 695 through information theory, 2024. URL <https://arxiv.org/abs/2411.11984>.

696

697 Hugo Touvron, Thibaut Lavril, Gautier Izacard, Xavier Martinet, Marie-Anne Lachaux, Timothée
 698 Lacroix, Baptiste Rozière, Naman Goyal, Eric Hambro, Faisal Azhar, et al. Llama: Open and
 699 efficient foundation language models. *arXiv preprint arXiv:2302.13971*, 2023.

700

701 Xuezhi Wang, Jason Wei, Dale Schuurmans, Quoc V Le, Ed H. Chi, Sharan Narang, Aakanksha
 702 Chowdhery, and Denny Zhou. Self-consistency improves chain of thought reasoning in language
 703 models. In *The Eleventh International Conference on Learning Representations*, 2023. URL
<https://openreview.net/forum?id=1PL1NIMMrw>.

702 Jason Wei, Xuezhi Wang, Dale Schuurmans, Maarten Bosma, brian ichter, Fei Xia, Ed Chi, Quoc V
 703 Le, and Denny Zhou. Chain-of-thought prompting elicits reasoning in large language models. In
 704 S. Koyejo, S. Mohamed, A. Agarwal, D. Belgrave, K. Cho, and A. Oh (eds.), *Advances in Neural*
 705 *Information Processing Systems*, volume 35, pp. 24824–24837. Curran Associates, Inc., 2022.

706 Yangzhen Wu, Zhiqing Sun, Shanda Li, Sean Welleck, and Yiming Yang. Scaling inference
 707 computation: Compute-optimal inference for problem-solving with language models. In
 708 *The 4th Workshop on Mathematical Reasoning and AI at NeurIPS’24*, 2024. URL <https://openreview.net/forum?id=j7DZWSc8qu>.

709

710 Yunhui Xia, Wei Shen, Yan Wang, Jason Klein Liu, Hufeng Sun, Siyue Wu, Jian Hu, and Xiaolong
 711 Xu. Leetcodedataset: A temporal dataset for robust evaluation and efficient training of code llms,
 712 2025. URL <https://arxiv.org/abs/2504.14655>.

713

714 Keyulu Xu, Jingling Li, Mozhi Zhang, Simon S Du, Ken-ichi Kawarabayashi, and Stefanie Jegelka.
 715 What can neural networks reason about? *arXiv preprint arXiv:1905.13211*, 2019.

716

717 Shunyu Yao, Dian Yu, Jeffrey Zhao, Izhak Shafran, Thomas L. Griffiths, Yuan Cao, and Karthik R
 718 Narasimhan. Tree of thoughts: Deliberate problem solving with large language models. In
 719 *Thirty-seventh Conference on Neural Information Processing Systems*, 2023. URL <https://openreview.net/forum?id=5Xc1ecx0lh>.

720

721 Tian Ye, Zicheng Xu, Yuanzhi Li, and Zeyuan Allen-Zhu. Physics of language models: Part 2.1,
 722 grade-school math and the hidden reasoning process, 2024. URL <https://arxiv.org/abs/2407.20311>.

723

724 Yizhou Zhang, Lun Du, Defu Cao, Qiang Fu, and Yan Liu. An examination on the effectiveness of
 725 divide-and-conquer prompting in large language models, 2024. URL <https://arxiv.org/abs/2402.05359>.

726

727 Denny Zhou, Nathanael Schärli, Le Hou, Jason Wei, Nathan Scales, Xuezhi Wang, Dale Schuurmans,
 728 Claire Cui, Olivier Bousquet, Quoc V Le, and Ed H. Chi. Least-to-most prompting enables complex
 729 reasoning in large language models. In *The Eleventh International Conference on Learning*
 730 *Representations*, 2023. URL <https://openreview.net/forum?id=WZH7099tgefM>.

731

732

733

734

735

736

737

738

739

740

741

742

743

744

745

746

747

748

749

750

751

752

753

754

755

756 757 758 759 760 761 762 763 764 765 766 767 768 769 770 771 772 773 774 775 776 777 778 779 780 781 782 783 784 785 786 787 788 789 790 791 792 793 794 795 796 797 798 799 800 801 802 803 804 805 806 807 808 809 Appendix

CONTENTS

A The Use of Large Language Models (LLMs)	16
B Formal Definitions of Simplified Arithmetic Problem	16
B.1 Problem Formulation	16
B.2 Contrast to vanilla arithmetic problem	17
C Dynamic Programming (DP) Problems	17
C.1 Experimental Setup	17
C.2 Evaluation of Dynamic-Programming Tasks on Larger Qwen2.5 Models	18
D Supplementary Details on Real world Experiment for Optimal CoT Length	18
D.1 Solution Length Control	18
D.2 Step Segmentation	19
D.3 More Details of Figure 2b.	19
D.4 On the Definition of Task Difficulty and Mitigating Accuracy Bias	20
E Looped Transformer	20
F Extended Experiments on Broader Domains	20
F.1 Additional Results for Figure 2b.	20
F.2 Experiments on the Full MATH500 Dataset	20
F.3 Experiments on the Winogrande Dataset	22
G Supplementary Details on Real World Experiment for RL Simplicity Bias	22
H Additional Synthetic Experiment Details	22
H.1 Training details	22
H.2 Observation of subtask loss	23
I Theoretical Results under Broader Scenarios	23
I.1 General Errors	23
I.2 Random Error	24
J Proof	24
J.1 Proof of Proposition 4.1	24
J.2 Proof of Theorem 4.2	25
J.3 Proof of Corollary 4.3	26
J.4 Proof of Theorem I.3	27

810	J.5	Proof of Theorem I.6	27
811	J.6	Proof of Corollary 4.4	28
812	J.7	Technical Lemmas	29
813			
814			
815			
816	K	Pseudo-code of Length-filtered Vote	31

K Pseudo-code of Length-filtered Vote 31

A THE USE OF LARGE LANGUAGE MODELS (LLMs)

In this work, LLMs are primarily employed for two purposes: (1) polishing the language of the manuscript to ensure grammatical correctness and coherence, and (2) assisting in the standardized organization and documentation of the released codebase. Importantly, all conceptual development, theoretical analysis, experimental design, and result interpretation are conducted independently by the authors. The use of LLMs is strictly limited to auxiliary tasks, ensuring that the scientific contributions of this paper remain entirely unaffected by such tools.

B FORMAL DEFINITIONS OF SIMPLIFIED ARITHMETIC PROBLEMS

To begin, we aim to empirically investigate the relationship between reasoning performance and CoT length. Therefore, we need to control a given model to generate reasoning chains of varying lengths for a specific task. Unfortunately, no existing real-world dataset or model fully meets these strict requirements. Real-world reasoning tasks, such as GSM8K or MATH (Cobbe et al., 2021; Hendrycks et al., 2021b), do not provide multiple solution paths of different lengths, and manually constructing such variations is challenging. Moreover, it is difficult to enforce a real-world model to generate question. Given these limitations, we begin our

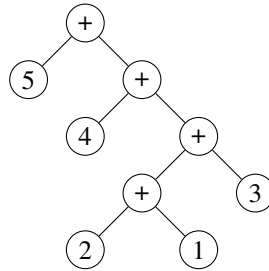


Figure 6: Computation tree of arithmetic expression $5 + (4 + ((2 + 1) + 3))$.

B.1 PROBLEM FORMULATION

To investigate the effect of CoT length in a controlled manner, we design a synthetic dataset of simplified arithmetic tasks with varying numbers of reasoning steps in the CoT solutions.

Definition B.1 (Problem). In a simplified setting, an arithmetic task q is defined as a binary tree of depth T . The root and all non-leaf nodes are labeled with the $+$ operator, while each leaf node contains a numerical value (mod 10). In addition, we impose a constraint that every non-leaf node must have at least one numerical leaf as a child.

The bidirectional conversion method between arithmetic expressions and computation trees is as follows: *keeping the left-to-right order of numbers unchanged, the computation order of each "+" or tree node is represented by tree structure or bracket structures*. For example, consider the task $5 + (4 + ((2 + 1) + 3))$ with $T = 4$. The corresponding computation tree is defined as Figure 6.

To ensure that CoT solutions of the same length have equal difficulty for a specific problem, we assume that each reasoning step performs the same operations within a single CoT process.

Definition B.2 (Solution). We define a t -hop CoT with a fixed each step length of t as a process that executes t operations starting from the deepest level and moving upward recursively.

According to this definition, the execution sequence is uniquely determined. For example, one way to solve expression in Figure 6 is by performing one addition at a time:

$$5 + (4 + ((2 + 1) + 3)) = <1> \quad (3)$$

$$2 + 1 = 3 \quad (4)$$

$$3 + 3 = 6$$

$$4 + 6 = 0$$

$$5 + 0 = 5 <\text{END}>.$$

Another approach is to perform two additions at a time:

$$5 + (4 + ((2 + 1) + 3)) = <2> \quad (5)$$

$$(2 + 1) + 3 = 6$$

$$5 + (4 + 6) = 5 <\text{END}>.$$

The latter approach is half as long as the former, but each reasoning step is more complex¹. This illustrates a clear trade-off between the difficulty of each subtask and the total number of reasoning steps.

In practice, when t does not evenly divide T , the final step performs $T \bmod t$ operations. To guide the model in generating the desired CoT length, we insert the control token $<\text{t}>$ after the question and before the beginning of the solution. To preserve the parentheses that indicate the order of operations, we construct expressions in Polish notation. However, for readability, we present each problem in its conventional form throughout the article.

B.2 CONTRAST TO VANILLA ARITHMETIC PROBLEM

Why pruning? Initially, we intended to create a synthetic dataset for regular arithmetic tasks, but we quickly realized that the computation tree for such tasks is uncontrollable. For example, consider the task $1 * 2 + 3 * 4$. We hoped to compute 2 operators in one step, but found it impossible because the addition needs to be computed after the two multiplications, and we cannot aggregate two multiplications in one subtask. Therefore, pruning the computation tree becomes essential.

Why only focusing on addition? There are two reasons why we focus on arithmetic tasks involving only addition: first, it simplifies pruning, as the order of operations can be controlled solely by parentheses; second, it facilitates the computation of sub-tasks, since parentheses do not affect the final result, and the model only needs to compute the sum of all the numbers when solving a sub-task. We aim for the model to handle longer sub-tasks, thereby allowing a broader study of the impact of CoT length.

Will the simplified synthetic dataset impact the diversity of the data? We need to clarify that even with pruning, the structure of the expressions will still vary because swapping the left and right child nodes of each non-leaf node in the computation tree results in different expressions. When $T > 30$, the number of possible variations exceeds 1×10^9 .

C DYNAMIC PROGRAMMING (DP) PROBLEMS

C.1 EXPERIMENTAL SETUP

To complement the arithmetic dataset, we design a classical dynamic programming (DP) problem — the **Maximum Path Sum in a Number Triangle**. This task shares the same desirable decomposability property as the arithmetic problems: it naturally admits multiple solutions of varying CoT lengths, making it suitable for analyzing the scaling behavior of reasoning length.

We construct a dataset of number triangles with varying heights H . Each triangle consists of H rows, where the i -th row contains i integers sampled uniformly from a predefined range (e.g., $[1, 99]$). The

¹This is because performing two operations at once requires the model to either memorize all combinations of numbers in a two-operator equation and their answers, apply techniques like commutativity to reduce memory requirements, or use its mental reasoning abilities to perform the two operations without relying on CoT.

total task difficulty is quantified by the number of rows H , since longer triangles require deeper reasoning chains to propagate information from the base to the top.

For example, consider the following triangle of height $H = 4$:

			7	
		3	8	
	8	1	0	
2	7	4	4	

The goal is to find a path from the apex (top) to the base that maximizes the sum of visited numbers. The canonical solution employs a bottom-up dynamic programming algorithm: starting from the second-to-last row, we update each entry as the sum of the current value and the maximum of its two children in the row below. Repeating this process row by row eventually yields the maximum path sum at the apex.

A long CoT solution might be designed to process $t = 1$ layer per step.

$$\begin{aligned}
 \text{Row 3 update: } & [8 + \max(2, 7), 1 + \max(7, 4), 0 + \max(4, 4)] \\
 & = [15, 8, 4] \\
 \text{Row 2 update: } & [3 + \max(15, 8), 8 + \max(8, 4)] \\
 & = [18, 16] \\
 \text{Row 1 update: } & [7 + \max(18, 16)] \\
 & = [25]
 \end{aligned}$$

A shorter CoT solution for the same problem might process $t = 2$ layers per step.

$$\begin{aligned}
 \text{Step 1 (Row 4} \rightarrow \text{Row 2): } & \begin{cases} \text{For Row 2, Col 1: } 3 + \max(2 + 8, 7 + 8) = 3 + \max(10, 15) = 18 \\ \text{For Row 2, Col 2: } 8 + \max(7 + 1, 4 + 1) = 8 + \max(8, 5) = 16 \end{cases} \\
 & \Rightarrow \text{Row 2 becomes } [18, 16]
 \end{aligned}$$

$$\text{Step 2 (Row 2} \rightarrow \text{Row 1): } 7 + \max(18, 16) = 7 + 18 = 25$$

Thus, the maximum path sum is 25.

C.2 EVALUATION OF DYNAMIC-PROGRAMMING TASKS ON LARGER QWEN2.5 MODELS

To further validate the non-triviality of our dynamic-programming (DP) benchmark and examine its behavior on stronger models, we evaluate Qwen2.5 instruct models of varying sizes on DP tasks of depths 6, 8, and 10. For each difficulty level, we generate 100 problem instances and sample 10 CoT responses per instance. Following our real-world evaluation protocol, we determine the *optimal CoT length* for each model–task pair by selecting the chain length that achieves highest accuracy.

We omit the 1.5B model from analysis due to its low performance (<10% accuracy). Importantly, even the 72B model does not achieve perfect accuracy on depth-6 tasks (81.8%), indicating that our DP benchmark remains *non-trivial* and effectively probes structured algorithmic reasoning.

Table 2 summarizes optimal CoT lengths and corresponding accuracies. Two clear trends emerge: 1) larger models consistently require *shorter* optimal CoT lengths, and 2) deeper DP tasks require *longer* optimal CoT lengths. Both findings are fully aligned with our theoretical predictions regarding adaptive CoT behavior with respect to model capability and task difficulty.

D SUPPLEMENTARY DETAILS ON REAL WORLD EXPERIMENT FOR OPTIMAL COT LENGTH

D.1 SOLUTION LENGTH CONTROL

To study the impact of CoT length on performance under a given problem difficulty, we need to induce the model to naturally generate solutions of varying lengths. Simply adding prompts like

972

Table 2: Optimal CoT length (accuracy %) across Qwen2.5 model sizes and DP task depths.

973

974

DP Depth	6	8	10
7B	5 (35.0%)	7 (30.3%)	8 (22.6%)
32B	4 (70.6%)	5 (45.8%)	8 (42.9%)
72B	3 (81.8%)	5 (66.7%)	6 (46.2%)

975

976

977

978

979

980

981

“please use 100 tokens to solve this problem” or “please use 10 steps to solve this problem” is not ideal because the model’s ability to follow instructions regarding output length is limited, and such fixed-length prompts may not ensure fairness across problems of different difficulties. Moreover, prompting for a specific length might lead the model to generate irrelevant tokens or steps just to “pad the length,” without actually changing the number of steps or the complexity of the reasoning. Additionally, controlling `max_length` is also problematic, as overly long responses might get truncated, which would directly lead to lower accuracy for longer outputs. What we really want is for the model to generate a complete and coherent long response on its own, so we can observe the corresponding accuracy.

990

991

992

993

994

995

996

D.2 STEP SEGMENTATION

997

998

999

1000

1001

1002

1003

1004

1005

Simply measuring CoT length by counting tokens is neither rigorous nor meaningful. Since our focus is on final performance rather than efficiency, we care more about using CoT length to reflect the complexity of the reasoning pattern. In this sense, the number of reasoning steps can serve as a more appropriate indicator of CoT length. As we discussed earlier, the step number captures how the model decomposes the problem, which directly reflects the complexity of its reasoning. In contrast, token length fails to capture this because, as the model thinks more deeply and the number of steps increases, the number of tokens per step may decrease—making the total token count unpredictable and unreliable as a proxy for reasoning complexity.

1006

1007

1008

1009

1010

1011

1012

1013

1014

1015

1016

1017

1018

When calculating the number of steps, we separate the full reasoning chain using “\n” (Fu et al., 2023) and remove empty lines caused by “\n\n”. Then we consider the total number of lines as the CoT length. Since questions in the MATH dataset are challenging and lead to high variability in final CoT lengths, we normalize the lengths by applying `length = length // bin_width`. For experiments comparing different models (e.g., optimal CoT length per model or optimal vs. longest CoT), the questions within each length bin differ, which introduces variability. To reduce this variance and ensure each bin has enough samples, we use a relatively large bin width of 5. In contrast, for analyzing the influence of task difficulty, where each calculation on optimal CoT length only contains one question, we adopt a finer bin width of 2 for better resolution (we also verified that using width 1 yields almost identical results).

1019

1020

1021

D.3 MORE DETAILS OF FIGURE 2B.

1022

1023

1024

1025

When evaluating the results, questions with accuracy < 0.01 or > 0.99 (indicating all incorrect or all correct responses) are excluded, as their accuracy does not vary with step length changes.

To better understand the reliability of the observed trend between task difficulty and optimal Chain-of-Thought (CoT) length, we compute a 95% confidence interval around the linear regression line. Specifically, we use standard methods based on the Student’s t-distribution to estimate uncertainty in the predicted values. The confidence band reflects how much the estimated mean CoT length is expected to vary given the finite sample size and the distribution of data points.

1026 D.4 ON THE DEFINITION OF TASK DIFFICULTY AND MITIGATING ACCURACY BIAS
10271028 Defining task difficulty requires particular care because raw accuracy can be biased by a model’s in-
1029 herent preference for certain CoT lengths. We address this issue using two complementary strategies.
10301031 **Controlling for CoT-Length Bias.** Different questions may elicit different preferred CoT lengths
1032 from the model, which can artificially inflate or deflate their measured difficulty. To reduce this
1033 confounding factor, for each question we explicitly prompt the model to generate *multiple* CoT
1034 lengths when producing the 60 responses used in our evaluation. This procedure minimizes the effect
1035 of internal length biases on accuracy and yields a more reliable task-difficulty signal.
10361037 **Model-Aware Difficulty Definition.** Task difficulty is inherently model-dependent: a problem that
1038 is easy for one model may be challenging for another due to differences in scale, data coverage, or
1039 training. For this reason, we define difficulty in a model-aware manner by using the *average accuracy*
1040 of the evaluated model as the difficulty indicator. This ensures that the difficulty metric faithfully
1041 reflects the model’s actual competence rather than relying on externally imposed or model-agnostic
1042 notions of hardness.
10431044 E LOOPED TRANSFORMER
10451046 Following Bae et al. (2025), we implement the looped Transformer architecture by iteratively applying
1047 a single Transformer layer multiple times. Specifically, we train two variants with `loops` = 6 and
1048 `loops` = 9, both configured with an embedding dimension of 64×9 and 9 attention heads (only
1049 4 MB parameters in total). Training is conducted on a mixed dataset with maximum task difficulty
1050 = 64 and maximum CoT hop size = 8. Detailed training procedures are provided in the released
1051 code.
10521053 F EXTENDED EXPERIMENTS ON BROADER DOMAINS
10541055 To strengthen the generality of our experimental conclusions, we expanded both the scale of the data
1056 and the diversity of reasoning domains considered. Specifically, we conducted experiments in the
1057 following three areas:
10581059

- **Mathematical reasoning:** We employed the full MATH500 dataset (Lightman et al., 2023).
1060 This dataset contains a curated subset of 500 problems from the original MATH benchmark.
- **Scientific reasoning:** We adopted the MMLU STEM (Hendrycks et al., 2021a) dataset,
1061 which is a subset of STEM subjects defined in the original MMLU benchmark, which covers
1062 a wide range of scientific and engineering domains.
- **Commonsense reasoning:** We used the full Winogrande (Sakaguchi et al., 2019) xs training
1063 split. This dataset formulates a fill-in-the-blank task with binary options, designed to require
1064 non-trivial commonsense reasoning.

10651066 F.1 ADDITIONAL RESULTS FOR FIGURE 2B.
10671068 Before presenting the results on additional datasets, we first further investigate the relationship
1069 between task difficulty and optimal CoT length on real-world benchmarks using different models.
1070 As shown in Figure 7, the findings are consistent and compelling: across all evaluated models, we
1071 observe a clear and statistically significant correlation between task difficulty and the corresponding
1072 optimal CoT length. These analyses are also validated on broader datasets such as MATH500,
1073 MMLU STEM, and WINOGRANDE.
10741075 F.2 EXPERIMENTS ON THE FULL MATH500 DATASET
10761077 We acknowledge the need for broader validation beyond a single subset of data. Therefore, we
1078 further conducted experiments on the complete MATH500 dataset. Specifically, we evaluated the
1079 Qwen2.5-Instruct models (1.5B, 7B, 32B, and 72B) with 30 sampled solutions per question.
1080

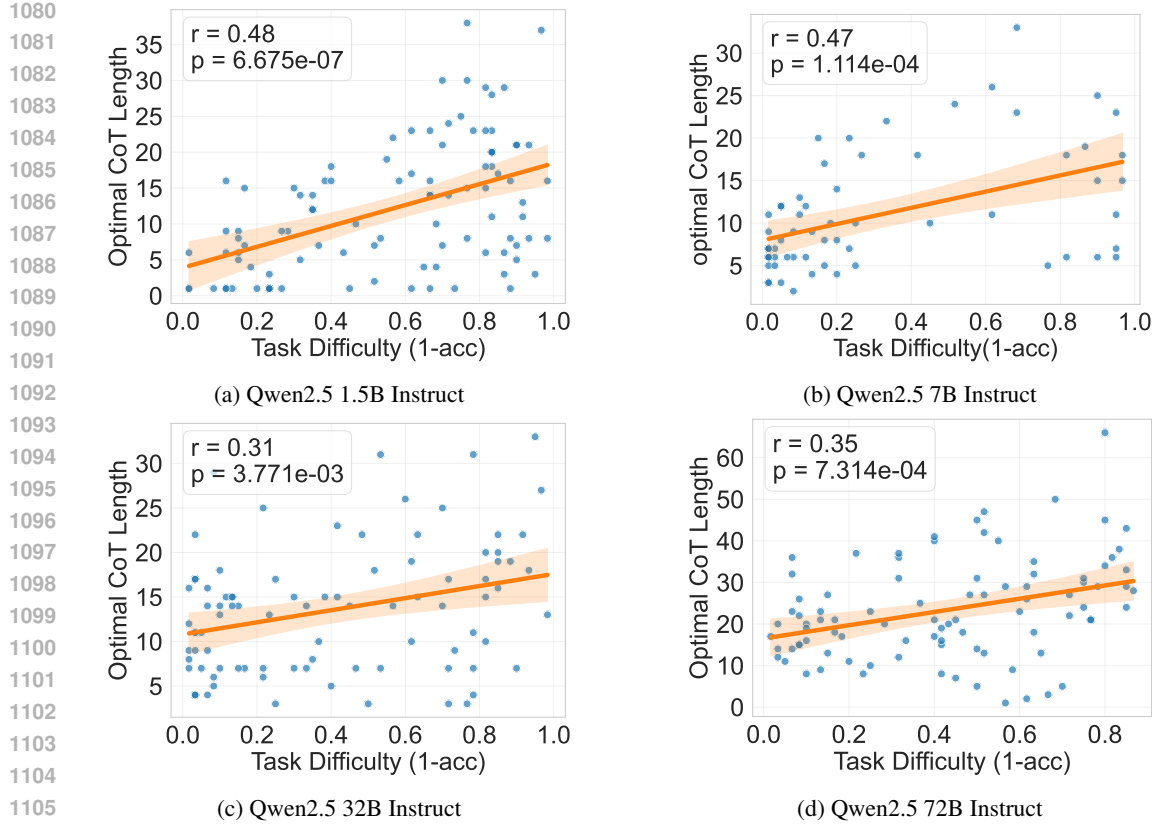


Figure 7: Evaluation between task difficulties and optimal CoT lengths on MMLU STEM datasets.

Table 3 reports the comparison of accuracy achieved with the longest chain-of-thought (CoT) versus the optimal CoT length, across different model sizes. Table 4 further examines the relationship between optimal CoT length and problem difficulty.

Table 3: Optimal CoT length vs. model size on the full MATH500 dataset.

	1.5B	7B	32B	72B
Accuracy (longest length)	0.18	0.27	0.40	0.08
Accuracy (optimal length)	0.38 (+0.20)	0.82 (+0.55)	0.81 (+0.41)	0.81 (+0.73)
Optimal length	5	2	1	2

Table 4: Correlation between optimal CoT length and task difficulty.

	1.5B	7B	32B	72B
<i>r</i>	0.2092	0.2378	0.2266	0.1986
<i>p</i>	0.0068	0.0034	0.0029	0.0297

In this experiment, where problem difficulty was not explicitly controlled, we observed that the 7B, 32B, and 72B models achieved peak performance at shorter CoT lengths. This trend is likely explained by the dataset's high concentration of easier problems (levels 1–4), which, as shown in our previous results, generally require shorter reasoning chains. By contrast, the much weaker 1.5B model still benefited from longer reasoning (optimal length = 5).

Importantly, despite the skewed distribution of problem difficulty, the key relationship we aimed to study remains intact: we consistently found a statistically significant correlation ($p < 0.05$)

1134 between task difficulty and optimal CoT length, which aligns with our earlier findings across all other
 1135 experiments.
 1136

1137 F.3 EXPERIMENTS ON THE WINOGRANDE DATASET

1139 We have also conducted new experiments on the WINOGRANDE (Sakaguchi et al., 2019) dataset to
 1140 assess commonsense reasoning. In particular, we evaluated the Qwen2.5-Instruct models (1.5B, 7B,
 1141 32B, and 72B) on the full WINOGRANDE-XS training split, replicating the experimental setup from
 1142 Figure 2 of our main paper.

1143 Table 5 reports the comparison between the longest and optimal CoT lengths across different model
 1144 sizes, while Table 6 shows the correlation between optimal CoT length and task difficulty.
 1145

1146 Table 5: Optimal CoT length vs. model size on the WINOGRANDE-XS dataset.
 1147

	1.5B	7B	32B	72B
Accuracy (longest length)	0.56	0.69	0.72	0.85
Accuracy (optimal length)	0.63 (+0.07)	0.74 (+0.05)	0.80 (+0.08)	0.93 (+0.08)
Optimal length	15	15	10	9

1153 Table 6: Correlation between optimal CoT length and task difficulty on WINOGRANDE-XS.
 1154

	1.5B	7B	32B	72B
r	0.2201	0.4256	0.3886	0.2098
p	0.0052	< 1e-4	0.0120	0.0077

1160 These experiments significantly broaden the generalizability of our conclusions. The results corroborate
 1161 our earlier findings from the mathematical domain, demonstrating that the optimal CoT length
 1162 decreases as the model size increases and that it remains significantly correlated with task difficulty
 1163 ($p < 0.05$).
 1164

1165 G SUPPLEMENTARY DETAILS ON REAL WORLD EXPERIMENT FOR RL 1166 SIMPLICITY BIAS

1168 For Figure 2c, we use Qwen2.5-7B-Instruct (Qwen et al., 2025) as the base model, Group Relative
 1169 Policy Optimization with R1-like prompting (Shao et al., 2024; Guo et al., 2025) for the reinforcement
 1170 learning process, and LeetCode-2K (Xia et al., 2025) as the training and evaluation dataset. We take
 1171 the following training configuration by default:
 1172

1173 Table 7: Hyperparameter settings for real-world RL experiments with Qwen2.5-instruct models.
 1174

Learning Rate	Max Epochs	Rollout Samples	Reverse KL Coefficient	Entropy Loss Coefficient	Effective Batch Size
5e-7	10	16	1e-3	5e-3	256

1178 H ADDITIONAL SYNTHETIC EXPERIMENT DETAILS

1180 H.1 TRAINING DETAILS

1182 In default, we train different models (layers ranging from 5 to 9) on the same dataset, which included
 1183 mixed questions with total operators $T \in [12, 80]$ and random sampled CoT solutions with each step
 1184 operators $t \in [1, 12]$. All other parameters are kept the same with the huggingface GPT-2 model.
 1185 During the training process, the CoT indicator token $\langle t \rangle$ is also trained, so that during test-time, we
 1186 can let the model decide which type of CoT it will use by only prompting the model with the question.
 1187 For each model, we train 25000 iterations with batch size that equals 256. During test-time, we test
 1188 100 questions for each T and t . All experiments can be conducted on one NVIDIA A800 80G GPU.
 1189

1188
1189

H.2 OBSERVATION OF SUBTASK LOSS

1190
1191
1192
1193

As we observed in training losses, the loss of subtask generation tokens (e.g. 1 + 2) for the easiest subtask ($t = 1$) is about 3 times larger than the hardest subtask ($t = 12$), while the loss ratio for subtask answer tokens is $1e4$. Therefore, it is acceptable for taking the subtask error rate constant with t .

1194
1195
1196
1197

Besides, there is no obvious pattern showing the model sizes affect the subtask loss. Moreover, the smallest model and the largest model have almost the same subtask loss. Therefore, in our settings, we take model size as irrelevant with the subtask error rate.

1198
1199

I THEORETICAL RESULTS UNDER BROADER SCENARIOS

1200
1201

I.1 GENERAL ERRORS

1202
1203
1204
1205
1206

In the simple case we discussed in Section 4, we discussed the trend of overall accuracy with respect to N and the variation of optimal N with M and T , assuming the subtask error rate is a linear function. In the following discussion, we aim to derive conclusions corresponding to more general error rate functions. We find that as long as the error function satisfies some basic assumptions on the **monotonicity** and **convexity** of the error functions, the above conclusions still hold.

1207

Assumption I.1. $E(N, M, T)$ satisfies the following reasonable conditions:

1208

- $0 < E(N = 1, M, T) < 1$
- $\lim_{N \rightarrow +\infty} E(N, M, T) = 0$
- $E(N, M, T)$ is monotonically decreasing with N , since more detailed decomposition leads to easier subtask.
- $E(N, M, T)$ is convex with N , since the benefits of further decomposing an already fine-grained problem (N is large) are less than the benefits of decomposing a problem that has not yet been fully broken down (N is small).
- $E(N, M, T)$ is monotonically decreasing with M , since stronger models have less subtask error rate.
- $E(N, M, T)$ is monotonically increasing with T , since harder total task leads to harder subtask while N, M are the same.

1209

Assumption I.2. $\sigma(T)$ is monotonically increasing with T

1210

With Assumption I.1 and I.2), the core insights from the linear case can be generalized.

1211

Theorem I.3. *For a noise function $0 < \sigma(T) < 1$ and a subtask error rate function $0 < E(N, M, T) < 1$ satisfying Assumptions I.1 and I.2, the general final accuracy function $A(N)$ from Proposition 4.1 has the following properties:*

1212

- $\lim_{N \rightarrow +\infty} A(N) = 0$. (Excessively long chains always fail.)
- If $A(N)$ has a maximum at $N^* > 1$, then N^* has a lower bound related to M and T :

1213
1214

$$N^* \geq N_{LB}(M, T) = E_N^{-1} \left(1 - \frac{1}{e^2(1 - \sigma(T))} ; M, T \right), \quad (6)$$

1215
1216

where $E_N^{-1}(\cdot; M, T)$ is the inverse of $E(N, M, T)$ with respect to N .

1217
1218
1219
1220
1221

The monotonicity of E_N^{-1} with respect to M (decreasing) and T (increasing, assuming $\sigma(T)$ doesn't dominate adversely) implies that the qualitative scaling laws (Corollaries stemming from Theorem 4.2) still hold under general conditions, supporting the empirically observed Simplicity Bias and the inverted U-shaped performance.

1222
1223
1224

Corollary I.4. *As the model becomes stronger, E^{-1} decreases monotonically with respect to M , which leads to a decrease of $N(M, T)$.*

1225
1226
1227

Corollary I.5. *As the task becomes harder, E^{-1} is monotonically increasing with respect to T , which leads to an increase in $N(M, T)$.*

1242 I.2 RANDOM ERROR
1243

1244 In Theorem 4.2 and I.3, we make a strong assumption that all sub-question or sub-answer errors are
1245 identical, which does not align well with real-world scenarios. In practice, each sub-task may exhibit
1246 a different error rate. However, they generally follow a trade-off: the more the task is decomposed,
1247 the easier each sub-task becomes. Specifically, we can model the error rate of each sub-task as a
1248 random variable with a fixed expectation that monotonically decreases with the number of CoT steps
1249 N .

1250 To simplify the problem, here we assume $\sigma_i \sim B(\alpha_1(T), \beta_1(T))$ to be the sub-question error rate,
1251 and $e_i \sim B(\alpha_2(N, M, T), \beta_2(N, M, T))$ to be the sub-answer error rate. Then, as a variant of
1252 Proposition 4.1, the expectation of final accuracy is $\mathbb{E} \left[\prod_{i=1}^N (1 - e_i)(1 - \sigma_i) \right]$.
1253

1254 It is worth noting that each σ_i or e_i is not independent. If most steps are easy (i.e., have low error
1255 rates), the remaining steps are more likely to be easy as well. Moreover, if a particular step serves as
1256 a self-validation step, its high accuracy can influence the correctness of other steps that depend on it.
1257 This also provides an interpretation for reasoning models exhibiting backtracking behavior.

1258 **Theorem I.6.** *Let $\alpha_1 = T$, $\beta_1 = C - T$, $\alpha_2 = T$, and $\beta_2 = NM - T$. Then the expected error
1259 rates for sub-questions and sub-answers are given by $\mathbb{E}[\sigma_i] = \frac{T}{C}$ and $\mathbb{E}[e_i] = \frac{T}{MN}$, respectively.
1260 Based on these estimates, we can derive an upper bound $\hat{A}(N)$ on the final accuracy*
1261

$$1262 \\ 1263 \mathbb{E} \left[\prod_{i=1}^N (1 - e_i)(1 - \sigma_i) \right] \leq \hat{A}(N) = \left[\left(1 - \frac{T}{C + 2N - 1} \right) \left(1 - \frac{T}{NM + 2N - 1} \right) \right]^N,$$

1267 which initially increases and then decreases as the number of CoT steps N grows.
1268

1269 This suggests that even with stochasticity, the fundamental trade-off leading to an optimal CoT length
1270 persists.
1271

1272 J PROOF
1273

1275 In this section, we provide the proofs for all theorems.
1276

1278 J.1 PROOF OF PROPOSITION 4.1
1279

1280 **Proposition 4.1.** *Assuming stepwise stationarity and independence conditioned on history, the final
1281 accuracy takes the form*

$$1283 A(N) = P(a_{final} = a_{final}^* \mid q, \theta, N) = \alpha \left((1 - \sigma(T)) (1 - E(N, M, T)) \right)^N, \quad (1)$$

1285 where α denotes a constant independent of N .
1286

1288 *Proof.* In each subtask t_i , which contains t operators, there are $2t + 1$ tokens (as the number of
1289 numerical tokens is one more than the number of operators). Therefore, the accuracy of each subtask
1290 is given by
1291

$$1292 P(t_i = t_i^* \mid H_{i-1}, q, \theta) = (1 - \sigma(T))^{2t+1}. \quad (7)$$

1294 In our theoretical analysis, for simplicity, we allow t to be a fraction, defined as $t = \frac{T}{N}$, and assume
1295 that each subtask has the same level of difficulty given T and N . Under this assumption, we have the

1296 final accuracy:
 1297

$$1298 \quad A(N) = P(a_N = a_N^* | q, \theta) \quad (8)$$

$$1299 \quad = \prod_{i=1}^N P(t_i = t_i^* | H_{i-1}, q, \theta) P(a_i = a_i^* | t_i, H_{i-1}, q, \theta) \quad (9)$$

$$1300 \quad = \prod_{i=1}^N (1 - \sigma(T))^{2t+1} (1 - E(N, M, T)) \quad (10)$$

$$1301 \quad = (1 - \sigma(T))^{N(2t+1)} (1 - E(N, M, T))^N \quad (11)$$

$$1302 \quad = (1 - \sigma(T))^{2T} ((1 - E(N, M, T))(1 - \sigma(T)))^N \quad (12)$$

$$1303 \quad = \alpha ((1 - E(N, M, T))(1 - \sigma(T)))^N \quad (13)$$

1304 \square
 1305
 1306
 1307
 1308
 1309
 1310
 1311
 1312

J.2 PROOF OF THEOREM 4.2

1313 **Theorem 4.2** (Optimal CoT length). *There exists an optimal $N^*(M, T)$ maximizing $A(N)$:*

$$1314 \quad N^*(M, T) = \frac{T Z}{M(Z+1)}, \quad Z = W_{-1}\left(-\left(1 - \frac{T}{Ce}\right)\right),$$

1315 where W_{-1} is the negative branch of the Lambert W function ($we^w = x$).
 1316
 1317
 1318

1319 *Proof.* Given Eq. (1) that
 1320

$$1321 \quad A(N) = \alpha \left(\left(1 - \frac{T}{C}\right) \left(1 - \frac{T}{NM}\right) \right)^N \quad (14)$$

1324 We consider function
 1325

$$1326 \quad f(x) = \left[\left(1 - \frac{T}{Mx}\right) \left(1 - \frac{T}{C}\right) \right]^x. \quad (15)$$

1327 For convenience, define
 1328

$$1329 \quad g(x) = \ln(f(x)) = x \ln\left[\left(1 - \frac{T}{Mx}\right) \left(1 - \frac{T}{C}\right)\right].$$

1330 Thus,
 1331

$$1332 \quad g'(x) = \left[\ln\left(1 - \frac{T}{Mx}\right) + \frac{T}{Mx \left(1 - \frac{T}{Mx}\right)} \right] + \ln\left(1 - \frac{T}{C}\right).$$

1333 Set $g'(x) = 0$:
 1334

$$1335 \quad \ln\left[\left(1 - \frac{T}{Mx}\right) \left(1 - \frac{T}{C}\right)\right] + \frac{T}{Mx \left(1 - \frac{T}{Mx}\right)} = 0.$$

1336 Let $A = \frac{1}{1 - \frac{T}{Mx}}$, then we have
 1337

$$1338 \quad \ln\left[\left(1 - \frac{T}{C}\right)\right] + A - 1 = \ln(A).$$

1339 Let $z := 1 - T/C$. (Since $T/C < 1$, $z = 1 - T/C > 0$.) By moving terms, we have:
 1340

$$1341 \quad -\frac{z}{e} = -A \exp(-A).$$

1350 Therefore,

1351
$$A = -W^{-1}\left(-\frac{z}{e}\right) = -Z,$$
 1352

1353 Finally, we have

1354

1355
$$N(M, T) = x = \frac{TZ}{M(Z+1)}$$
 1356

1357 Here $W(\cdot)$ is the **Lambert W function**, and for $0 < 1 - \frac{T}{C} < 1$, the argument $\alpha = -\frac{1-T/C}{e}$ lies in 1358 the interval $(-\frac{1}{e}, 0)$. This means there are two real branches W_0 and W_{-1} in that domain, but since 1359 $\frac{Z}{Z+1} > 0$, we have $Z < -1$. Therefore, we only take the solution on branch W_{-1} . \square 1360

1361

1362 J.3 PROOF OF COROLLARY 4.3

1363

1364 **Corollary 4.3** (Scaling laws). *From Theorem 4.2:*

1365

- $N^*(M, T)$ increases with T (harder tasks warrant longer CoT).
- The optimal operators per step $t^* = T/N^*(M, T) = M(1 + 1/Z)$ increases with T (envelope behavior).
- $N^*(M, T)$ decreases with M (stronger models need fewer steps).

1370

1371 *Proof.* The second and third conclusions can be easily derived through monotonic composition, so 1372 we primarily focus on proving the first point. We begin the proof by incorporating the notation from 1373 J.2. We have

1374
$$g'(x) = \left[\ln\left(1 - \frac{T}{Mx}\right) + \frac{T}{Mx\left(1 - \frac{T}{Mx}\right)} \right] + \ln\left(1 - \frac{T}{C}\right),$$
 1375

1376 and $x^*(T)$ such that $g'(x^*(T)) = 0$.1377 Let $F(x^*(T), T) = g'(x^*(T)) = 0$. We want to see how $x^*(T)$ changes as T changes, therefore we 1378 take total derivative w.r.t. T . By the chain rule,

1379
$$0 = \frac{d}{dT} F(x^*(T), T) = \underbrace{\frac{\partial F}{\partial x}(x^*(T), T) \cdot \frac{\partial x^*}{\partial T}(T)}_{\text{call this } F_x} + \underbrace{\frac{\partial F}{\partial T}(x^*(T), T)}_{\text{call this } F_T}.$$
 1380

1381 Hence

1382
$$\frac{\partial x^*}{\partial T}(T) = -\frac{F_T(x^*(T), T)}{F_x(x^*(T), T)}.$$
 1383

1384 So the sign of $x'^*(T)$ is the opposite of the sign of F_T , provided $F_x \neq 0$.

1385

1386 Since

1387
$$F_x(x, T) = -\frac{T^2}{x(Mx - T)^2} < 0, \forall x > 0, \quad (16)$$
 1388

1389 all we need to prove is

1390

1391
$$F_T(x^*(T), T) = \frac{T}{(Mx^*(T) - T)^2} - \frac{1}{C - T} > 0. \quad (17)$$
 1392

1393 That is

1394

1395
$$\frac{\sqrt{T(C-T)} + T}{M} > x^*(T). \quad (18)$$
 1396

1397

1398 Let $x_0(T) = \frac{\sqrt{T(C-T)} + T}{M}$ be the test point.

1399

1404 According to Lemma J.1, $F(x_0(T), T) < 0$. Since $F(x^*(T), T) = 0$, and $F_x(x^*(T), T) < 0$, we
 1405 have $x_0(T) > x^*(T)$.
 1406

1407 Thus, $F_T(x^*(T), T) > 0$ holds and we have proved our corollary with $\frac{\partial x^*}{\partial T}(T) > 0$.
 1408

□

1411 **J.4 PROOF OF THEOREM I.3**
 1412

1413 **Theorem I.3.** *For a noise function $0 < \sigma(T) < 1$ and a subtask error rate function $0 <$
 1414 $E(N, M, T) < 1$ satisfying Assumptions I.1 and I.2, the general final accuracy function $A(N)$
 1415 from Proposition 4.1 has the following properties:*

- $\lim_{N \rightarrow +\infty} A(N) = 0$. (Excessively long chains always fail.)
- If $A(N)$ has a maximum at $N^* > 1$, then N^* has a lower bound related to M and T :

$$1420 \quad N^* \geq N_{LB}(M, T) = E_N^{-1} \left(1 - \frac{1}{e^2(1 - \sigma(T))}; M, T \right), \quad (6)$$

1422 where $E_N^{-1}(\cdot; M, T)$ is the inverse of $E(N, M, T)$ with respect to N .
 1423

1424 *Proof.* (1) Since $0 < A(N) < (1 - \sigma(T))^N$, and $\lim_{N \rightarrow +\infty} (1 - \sigma(T))^N = 0$,
 1425 $\lim_{N \rightarrow +\infty} A(N, M, T) = 0$

1426 (2) Let $g(x)$ denote $E(x, M, T)$ and define $f(x) = \ln A(x)$. Then,

$$1429 \quad f'(x) = \ln(1 - \sigma(T)(1 - g(x))) - \frac{xE'(x)}{1 - E(x)} \quad (19)$$

$$1431 \quad < \ln(1 - \sigma(T)(1 - g(x))) + 2, \quad (\text{since } E \text{ is convex and } x = N \geq 1) \quad (20)$$

1432 If $A(N)$ attains its maximum at some point $N^* > 1$, then $\ln(1 - \sigma(T)) + 2 > 0$. Otherwise, we
 1433 would have $f'(x) < \ln(1 - \sigma(T)) + 2 \leq 0 \forall x > 1$, leading to a contradiction.
 1434

1435 Thus, it follows that $e^2(1 - \sigma(T)) > 1$.

1436 Now, define $N(M, T) = E^{-1} \left(1 - \frac{1}{e^2(1 - \sigma(T))} \right)$, which satisfies

$$1439 \quad \ln(1 - \sigma(T)(1 - g(N(M, T)))) + 2 = 0.$$

1440 If there exists $x^* < N(M, T)$ such that $f'(x^*) = 0$, then we obtain

$$1441 \quad 0 = f'(x^*) < \ln(1 - \sigma(T)(1 - E(x))) + 2 < 0,$$

1443 which is a contradiction. Hence, the assumption that $x^* < N(M, T)$ must be false.
 1444

1445 Therefore, we conclude that $x^* = N^* > N(M, T)$.
 1446

□

1448 **J.5 PROOF OF THEOREM I.6**
 1449

1450 **Theorem I.6.** *Let $\alpha_1 = T$, $\beta_1 = C - T$, $\alpha_2 = T$, and $\beta_2 = NM - T$. Then the expected error
 1451 rates for sub-questions and sub-answers are given by $\mathbb{E}[\sigma_i] = \frac{T}{C}$ and $\mathbb{E}[e_i] = \frac{T}{MN}$, respectively.
 1452 Based on these estimates, we can derive an upper bound $\hat{A}(N)$ on the final accuracy*

$$1454 \quad \mathbb{E} \left[\prod_{i=1}^N (1 - e_i)(1 - \sigma_i) \right] \leq \hat{A}(N) = \left[\left(1 - \frac{T}{C + 2N - 1} \right) \left(1 - \frac{T}{NM + 2N - 1} \right) \right]^N,$$

1455 which initially increases and then decreases as the number of CoT steps N grows.
 1456

1457

1458 *Proof.* According to the multidimensional version of Hölder's inequality,
 1459

$$1460 \quad \mathbb{E} \left[\prod_{i=1}^N (1 - e_i)(1 - \sigma_i) \right] \leq \prod_{i=1}^N (\mathbb{E}[(1 - e_i)^{2N}] \mathbb{E}[(1 - \sigma_i)^{2N}])^{\frac{1}{2N}} \quad (21)$$

$$1463 \quad (\text{Lemma J.2}) \leq \prod_{i=1}^N \left(1 - \frac{T}{C + 2N - 1} \right) \left(1 - \frac{T}{NM + 2N - 1} \right) \quad (22)$$

$$1466 \quad = \left[\left(1 - \frac{T}{C + 2N - 1} \right) \left(1 - \frac{T}{NM + 2N - 1} \right) \right]^N \quad (23)$$

1468 \square

1470 J.6 PROOF OF COROLLARY 4.4

1471 **Corollary 4.4** (RL Converges to Optimal CoT Length). *For gradient ascent on $J(\theta)$ with sufficiently
 1472 small step size, the policy converges to a deterministic solution $\pi_\theta(N_i) = 1$ iff $i = \arg \max_j A(N_j)$.
 1473 Thus, RL training converges to the optimal CoT length $N^* = \arg \max_{N \in \mathcal{A}} A(N)$.*

1474 *Proof.* We treat the choice of CoT length as a k -armed stochastic bandit with action set $\mathcal{A} =$
 1475 $\{N_1, \dots, N_k\}$ and unknown success probabilities² $A(N_i) \in (0, 1)$. Without loss of generality,
 1476 relabel the arms so that

$$1477 \quad A(N_1) = \max_j A(N_j) =: A^*, \quad A(N_1) \geq A(N_2) \geq \dots \geq A(N_k).$$

1478 The agent uses a softmax (Gibbs) policy

$$1479 \quad \pi_\theta(N_i) = \frac{e^{\theta_i}}{\sum_{j=1}^k e^{\theta_j}}, \quad \theta \in \mathbb{R}^k, \quad (24)$$

1480 and maximises the expected reward

$$1481 \quad J(\theta) = \sum_{i=1}^k \pi_\theta(N_i) A(N_i). \quad (25)$$

1482 Because π_θ is C^∞ in θ and $A(N_i)$ are constants, J is smooth.

1483 Under the REINFORCE estimator with sufficiently small, fixed step size $\eta > 0$, gradient ascent
 1484 updates take the form

$$1485 \quad \theta^{(t+1)} = \theta^{(t)} + \eta \nabla_\theta J(\theta^{(t)}), \quad (26)$$

1486 where

$$1487 \quad \frac{\partial J}{\partial \theta_i} = \pi_\theta(N_i) (A(N_i) - J(\theta)). \quad (27)$$

1488 Eq. (27) is the classical **replicator** (or logit) gradient. Define the simplex $\Delta^{k-1} := \{\pi \in (0, 1]^k \mid$
 1489 $\sum_i \pi_i = 1\}$ and write $\pi_\theta = (\pi_\theta(N_1), \dots, \pi_\theta(N_k))$.

1490 Letting $\eta \rightarrow 0$ yields the ODE

$$1491 \quad \dot{\pi}_i = \pi_i (A(N_i) - \langle \pi, A \rangle), \quad i = 1, \dots, k, \quad (28)$$

1492 with $\langle \pi, A \rangle = \sum_j \pi_j A(N_j)$. Eq. (28) is the **replicator dynamics** for a fitness landscape A on Δ^{k-1} .

1493 Consider the Kullback–Leibler divergence to the optimal pure strategy $\mathbf{e}_1 = (1, 0, \dots, 0)$,

$$1494 \quad V(\pi) = \sum_{i=1}^k \pi_i \ln \left(\frac{\pi_i}{e_{1,i}} \right) = -\ln \pi_1.$$

1500 ²By Proposition 4.1, $A(N_i)$ is the probability that the final answer is correct when a chain of length N_i is
 1501 used. The bandit is *stationary* because $A(N_i)$ does not depend on time or the agent's past actions.

1512 V is non-negative on Δ^{k-1} and $V(\pi) = 0$ iff $\pi = \mathbf{e}_1$.
 1513

1514 Taking the time derivative along Eq. (28) gives

$$1515 \quad \frac{dV}{dt} = -\frac{\dot{\pi}_1}{\pi_1} = -(A(N_1) - \langle \pi, A \rangle) \leq 0,$$

1517 with equality iff $\pi_1 = 1$ or $A(N_1) = \langle \pi, A \rangle$. The latter can only happen if $\pi_1 = 1$ because $A(N_1) >$
 1518 $A(N_j)$ for $j > 1$. Hence V is a strict Lyapunov function, and \mathbf{e}_1 is the *unique* asymptotically stable
 1519 equilibrium of Eq. (28). All other stationary points (mixtures over sub-optimal arms) are unstable.
 1520

1521 For sufficiently small but fixed η (choose $\eta < \frac{1}{A^+}$, which always exists), projected gradient ascent is
 1522 a *perturbed* discretisation of Eq. (28). Standard results for primal-space mirror descent imply that the
 1523 discrete iterates $\pi^{(t)} \equiv \pi_{\theta^{(t)}}$ converge almost surely to the set of asymptotically stable equilibria of
 1524 the ODE, i.e. to $\{\mathbf{e}_1\}$. Therefore

$$1525 \quad \lim_{t \rightarrow \infty} \pi_{\theta^{(t)}}(N_i) = \begin{cases} 1, & \text{if } i = \arg \max_j A(N_j), \\ 0, & \text{otherwise.} \end{cases}$$

1528 Because A may attain its maximum at several arms, the limit is a deterministic policy that places all
 1529 probability on *some* maximiser of A .

1530 Thus gradient ascent on Eq. (25) converges to a deterministic policy that always selects an optimal
 1531 CoT length $N^* = \arg \max_{N \in \mathcal{A}} A(N)$, completing the proof. \square
 1532

1533 J.7 TECHNICAL LEMMAS

1535 **Lemma J.1** (test point). *Let $F(x)$ be defined as*

$$1537 \quad F(x) = \ln \left(1 - \frac{T}{Mx} \right) + \frac{T}{Mx \left(1 - \frac{T}{Mx} \right)} + \ln \left(1 - \frac{T}{C} \right),$$

1539 where $T, M, C \in \mathbb{R}^+$ satisfy the conditions:

- 1541 • $0 < \frac{T}{C} < 0.9$,
- 1542 • $0 < \frac{T}{Mx} < 1$.

1544 Define x_0 as

$$1546 \quad x_0 = \frac{\sqrt{T(C-T)} + T}{M}.$$

1548 Then, we have

$$1549 \quad F(x_0) < 0.$$

1550 *Proof.* At $x = x_0$, note that

$$1552 \quad Mx_0 = \sqrt{T(C-T)} + T.$$

1553 Thus,

$$1555 \quad 1 - \frac{T}{Mx_0} = 1 - \frac{T}{T + \sqrt{T(C-T)}} = \frac{\sqrt{T(C-T)}}{T + \sqrt{T(C-T)}}.$$

1557 Therefore,

$$1559 \quad \ln \left(1 - \frac{T}{Mx_0} \right) = \ln \left(\frac{\sqrt{T(C-T)}}{T + \sqrt{T(C-T)}} \right) = \ln \sqrt{T(C-T)} - \ln(T + \sqrt{T(C-T)}).$$

1562 Also, observe that

$$1564 \quad \frac{T}{Mx_0 \left(1 - \frac{T}{Mx_0} \right)} = \frac{T}{(T + \sqrt{T(C-T)}) \left(\frac{\sqrt{T(C-T)}}{T + \sqrt{T(C-T)}} \right)} = \frac{T}{\sqrt{T(C-T)}} = \sqrt{\frac{T}{C-T}}.$$

1566 It is convenient to introduce the change of variable
 1567

$$1568 \quad 1569 \quad u = \sqrt{\frac{T}{C-T}},$$

1570 so that

$$1571 \quad T = u^2(C-T), \quad \sqrt{T(C-T)} = u(C-T).$$

1572 Then we have

$$1574 \quad T + \sqrt{T(C-T)} = u^2(C-T) + u(C-T) = u(C-T)(u+1).$$

1576 In these terms we have:

$$1577 \quad \ln \sqrt{T(C-T)} = \ln[u(C-T)] = \ln u + \ln(C-T),$$

$$1579 \quad \ln(T + \sqrt{T(C-T)}) = \ln[u(C-T)(u+1)] = \ln u + \ln(C-T) + \ln(u+1),$$

1580 and

$$1581 \quad 1582 \quad \sqrt{\frac{T}{C-T}} = u.$$

1584 Finally, we have

$$1585 \quad \ln\left(1 - \frac{T}{C}\right) = -\ln\left(\frac{C}{C-T}\right) = -\ln(u^2 + 1)$$

1587 Thus, the function $F(x_0)$ becomes

$$1589 \quad F(x_0) = \ln u + \ln(C-T) - (\ln u + \ln(C-T) + \ln(u+1)) + u - \ln(u^2 + 1) \quad (29)$$

$$1590 \quad = -\ln(u+1) + u - \ln(u^2 + 1), \quad (30)$$

1592 where $u = \sqrt{\frac{T}{C-T}} \in (0, 3)$. It is easy to show $F(x_0) < 0$ when $u \in (0, 3)$. \square
 1593

1594 **Lemma J.2** (Estimation of the n -th Moment of the Beta Distribution). *Let $x \sim \text{Beta}(\alpha, \beta)$. Then*

$$1595 \quad 1596 \quad \mathbb{E}[(1-x)^n] \leq \left(1 - \frac{\alpha}{\alpha + \beta + n - 1}\right)^n.$$

1598 *Proof.*

$$\begin{aligned} 1600 \quad \mathbb{E}[(1-x)^n] &= \frac{1}{B(\alpha, \beta)} \int_0^1 (1-x)^n x^{\alpha-1} (1-x)^{\beta-1} dx \\ 1601 \\ 1602 &= \frac{1}{B(\alpha, \beta)} \int_0^1 x^{\alpha-1} (1-x)^{\beta+n-1} dx \\ 1603 \\ 1604 &= \frac{B(\alpha, \beta+n)}{B(\alpha, \beta)} \\ 1605 \\ 1606 &= \frac{\Gamma(\alpha)\Gamma(\beta+n)}{\Gamma(\alpha+\beta+n)} \cdot \frac{\Gamma(\alpha+\beta)}{\Gamma(\alpha)\Gamma(\beta)} \\ 1607 \\ 1608 &= \frac{\Gamma(\beta+n)}{\Gamma(\beta)} \cdot \frac{\Gamma(\alpha+\beta)}{\Gamma(\alpha+\beta+n)} \\ 1609 \\ 1610 &= \prod_{i=0}^{n-1} \frac{\beta+i}{\alpha+\beta+i} \\ 1611 \\ 1612 &\leq \left(\frac{\beta+n-1}{\alpha+\beta+n-1} \right)^n \\ 1613 \\ 1614 &= \left(1 - \frac{\alpha}{\alpha+\beta+n-1} \right)^n. \end{aligned}$$

\square

1620 **K PSEUDO-CODE OF LENGTH-FILTERED VOTE**
16211622 **Algorithm 1** Length-filtered Vote

1624 1: **Input:** Model f_θ , Question q , Space of All Possible Answers A , Number of Total Groups M ,
1625 Number of Selected Groups K , Group Width D
1626 2: **Output:** Final Answer \hat{a}
1627 3: Sample candidates $c_1, \dots, c_n \stackrel{i.i.d.}{\sim} f_\theta(q)$
1628 4: **Define** $\mathcal{A}(c)$ as the corresponding answer of candidates c .
1629 5: **Define** $p_j \in [0, 1]^{|\mathcal{A}|}$ as the frequency of each answer in length group L_j .
1630 6: **for** $j = 1$ to m **do**
1631 $L_j = \{c_i \mid \ell(c_i) \in [D * (j - 1), D * j), i = 1, \dots, n\}$
1632 7: **for** $a \in \mathcal{A}$ **do**
1633 $p_j[a] = \frac{\sum_{c \in L_j} \mathbb{I}(\mathcal{A}(c) = a)}{|L_j|}$
1634
1635 8: **end for**
1636 9: **end for**
1637 10: $\{s_1, \dots, s_K\} = \arg \min_{S \subseteq \{1, \dots, M\}, |S|=K} \sum_{s \in S} H(p_s)$
1638 11: $\hat{a} = \arg \max_{a \in A} \sum_{c \in L_{s_1} \cup \dots \cup L_{s_K}} \mathbb{I}(\mathcal{A}(c) = a)$
1639 12: **return** \hat{a}

1640
1641
1642
1643
1644
1645
1646
1647
1648
1649
1650
1651
1652
1653
1654
1655
1656
1657
1658
1659
1660
1661
1662
1663
1664
1665
1666
1667
1668
1669
1670
1671
1672
1673